Received: 13 October 2016 | Accepted: 2 February 2017

DOI: 10.1111/gcb.13666

PRIMARY RESEARCH ARTICLE

WILEY Global Change Biology

Phenotypic distribution models corroborate species distribution models: A shift in the role and prevalence of a dominant prairie grass in response to climate change

Adam B. Smith[1] | Jacob Alsdurf[2] | Mary Knapp[3] | Sara G. Baer[4] | Loretta C. Johnson[2]

[1]Center for Conservation and Sustainable Development, Missouri Botanical Garden, St Louis, MO, USA

[2]Division of Biology, Kansas State University, Manhattan, KS, USA

[3]Weather Data Library, Kansas State University, Manhattan, KS, USA

[4]Department of Plant Biology and Center for Ecology, Southern Illinois University Carbondale, Carbondale, IL, USA

Correspondence
Adam B. Smith, Center for Conservation and Sustainable Development, Missouri Botanical Garden, St Louis, MO, USA.
Email: adam.smith@mobot.org

Funding information
U.S. Department of Agriculture, Grant/Award Number: 2008-3510004545; Kansas Academy of Science; Alan Graham Fund in Global Change.

Abstract

Phenotypic distribution within species can vary widely across environmental gradients but forecasts of species' responses to environmental change often assume species respond homogenously across their ranges. We compared predictions from species and phenotype distribution models under future climate scenarios for *Andropogon gerardii*, a widely distributed, dominant grass found throughout the central United States. Phenotype data on aboveground biomass, height, leaf width, and chlorophyll content were obtained from 33 populations spanning a ~1000 km gradient that encompassed the majority of the species' environmental range. Species and phenotype distribution models were trained using current climate conditions and projected to future climate scenarios. We used permutation procedures to infer the most important variable for each model. The species-level response to climate was most sensitive to maximum temperature of the hottest month, but phenotypic variables were most sensitive to mean annual precipitation. The phenotype distribution models predict that *A. gerardii* could be largely functionally eliminated from where this species currently dominates, with biomass and height declining by up to ~60% and leaf width by ~20%. By the 2070s, the core area of highest suitability for *A. gerardii* is projected to shift up to ~700 km northeastward. Further, short-statured phenotypes found in the present-day short grass prairies on the western periphery of the species' range will become favored in the current core ~800 km eastward of their current location. Combined, species and phenotype models predict this currently dominant prairie grass will decline in prevalence and stature. Thus, sourcing plant material for grassland restoration and forage should consider changes in the phenotype that will be favored under future climate conditions. Phenotype distribution models account for the role of intraspecific variation in determining responses to anticipated climate change and thereby complement predictions from species distributions models in guiding climate adaptation strategies.

KEYWORDS
biomass, climate change, intraspecific variation, local adaptation, phenotype distribution model, phenotypic variation, precipitation, species distribution model

1 | INTRODUCTION

Although local adaptation is commonly observed, species are often treated as functionally homogenous units when predicting responses to global change (Behrman, Keitt & Kiniry, 2014; Hällfors et al., 2016). Local adaptation arises from selective regimes that vary across an environmental gradient (Joshi et al., 2001; Linhart & Grant, 1996). Although local adaptation can enhance fitness under current conditions, it could serve as a liability during periods of environmental change if local adaptation reduces each population's niche breadth. In this situation, the persistence of locally adapted populations could be threatened if they are unable to respond in situ to changing conditions through rapid selection (Shaw & Etterson, 2012), phenotypic plasticity (Jump & Peñuelas 2005), or dispersal. Thus, incorporating intraspecific phenotypic variation in climate vulnerability analyses is an important challenge in predicting population responses to global change (Wittmann, Barnes, Jerde, Jones & Lodge, 2016).

Several approaches have been used to address the role of intraspecific variation in determining species' responses to global change. Most of these methods rely on splitting species into distinct genotypes or ecotypes, modeling each unit as if it were a different species, then aggregating the separate models (e.g., Hällfors et al., 2016). Many of these studies have found that accounting for intraspecific variation produces very different outcomes compared with more simplistic scenarios that assume species respond homogenously across populations. This method is appropriate for species that exhibit distinct populations, but may be inappropriate for species that span environmental gradients and show clinal phenotypic change (Clausen, Keck & Hiesey, 1940; Etterson, 2004; McMillan, 1959). An alternative approach is to account for intraspecific variation directly using models that predict performance in new environments based on environmental differences between 'home' and 'away' habitats (e.g., Behrman et al., 2014). Although powerful, this method requires reciprocal common garden experiments to calibrate models, and with a few exceptions, has typically only been applied to economically valuable plant species such as trees (Behrman et al., 2014; Benito-Garzón, Ruiz-Benito & Zavala, 2013). A third approach is to use models that capture the response of a phenotypic variable (i.e. a trait) as a function of environmental conditions. These 'phenotypic distribution models' [(PDMs) sensu Michel, Chien, Beachum, Bennett & Knouft, 2017; hereafter 'PDMs'] provide a richer depiction of a species' gradual phenotypic cline in response to environmental change. With the exception of phenological modeling, this type of approach has seldom been applied in the context of global change (Michel et al., 2017).

Andropogon gerardii Vitman (Big Bluestem) is a widely studied, ecologically important, warm-season (C_4) grass distributed throughout the central grasslands of North America (Weaver & Fitzpatrick, 1932). Predicting this species' response to climate change is important because *A. gerardii* can comprise up to 80% of biomass in the tallgrass prairie (Rogler, 1944); plays a key role in determining the structure of natural (Collins & Calabrese, 2012) and restored (Baer, Blair & Collins, 2016) tallgrass prairie communities; is a major forage source for livestock and wildlife (Rogler, 1944); and has promise for bioenergy production (Zhang, Johnson, Vara Prasad, Pei & Wang, 2015). The conservation and agricultural importance of *A. gerardii* has led to many studies of this species' phenotypic and genetic responses to climatic variation (phenotype: McMillan, 1959; Epstein, Lauenroth, Burke & Coffin, 1996; Epstein, Laurenroth, Burke & Coffin, 1998; Silletti & Knapp, 2002; Madakadze, Stewart, Madakadze & Smith, 2003; Kakani & Reddy, 2007; Collins et al., 2012; Mendola, Baer, Johnson & Maricle, 2015; and many others; genetic: Rouse et al., 2011; Gray et al., 2014; and others). Many studies demonstrate that drier conditions reduce the biomass and stature of *A. gerardii*. In contrast, *A. gerardii*'s phenotypic response to higher temperature is more idiosyncratic, either increasing (Kakani & Reddy, 2007), decreasing (Silletti & Knapp, 2002), responding unimodally (Madakadze et al., 2003), or not responding at all (Epstein et al., 1996), although the direction of the response may depend on initial temperature. Consistent with these observations, *A. gerardii* increases in stature and productivity with increasing precipitation (Epstein et al., 1996; Johnson et al., 2015; McMillan, 1959; Olsen, Caudle, Johnson, Baer & Maricle, 2013). Tellingly, a reciprocal common garden experiment established across a ~1200 km transect from western Kansas to Illinois demonstrated local adaptation and strong genetic control over growth-related traits in this species (e.g., biomass, height; Johnson et al., 2015; Mendola et al., 2015). The strong correlation between growth and climatic gradients (Gray et al., 2014; McMillan, 1959) suggests that adaptive, genetically controlled phenotypic differences could play an important role in predicting the distribution of *A. gerardii* in response to climate change.

The North American central grasslands are expected to experience greater variability in climate, including higher temperatures and increased frequency and severity of drought in the coming century (Polley et al., 2013). Our objective was to compare predictions from a species distribution model (SDM) trained using >5,000 herbarium specimen records to PDMs using the same climate variables and population-level measures of individual plant biomass, height, leaf width, and photosynthetic capacity of plants grown under common conditions in a greenhouse. We focused on data from the current core of the species' range in the central grasslands. Within the middle of the central grasslands, *A. gerardii* is the dominant tallgrass species (McMillan, 1959), whereas it is sub-dominant in the western and northern peripheries of the central grasslands. We also compared the relative importance of climate variables to the distribution of the species and its phenotype.

2 | MATERIALS AND METHODS

2.1 | Environmental data

We used 10-arcmin climate predictors obtained from the WORDLCLIM data set as predictors in the SDM and PDMs (Hijmans, Cameron, Parra, Jones & Jarvis, 2005). Current climate conditions were represented by average values over 1950–2000 and future

periods by ensemble averages of eight global circulation models (Table S1) centered on 2070 (2061–2080) for each of two greenhouse gas emissions pathways (IPCC scenarios RCP4.5 and RCP8.5), which bracket the most likely emissions pathways. RCP4.5 represents moderately strong abatement of the rate of greenhouse gas emissions, while RCP8.5 represents no abatement. Variables were selected from a larger set including the 19 BIOCLIM variables, BIOCLIM-like climatic water balance variables (difference between precipitation and potential evapotranspiration), precipitation of the establishment, and primary growing season (generally April-June), and total annual potential incoming solar radiation. Of these variables, we chose those that we expected exert direct control on the distribution and life cycle of *A. gerardii* (see Johnson et al., 2015; Madakadze et al., 2003; McMillan, 1959), and within those we selected variables with low pairwise correlations ($|\rho| < 0.7$). The SDMs and PDMs were trained with the five predictors we selected in this process: maximum temperature of the warmest month, mean monthly temperature range, annual temperature range, mean annual precipitation, and annual solar radiation. We also explored using growing season climatic water balance and growing season precipitation (which were all highly correlated), but results were qualitatively similar so we retained mean annual precipitation.

2.2 | Phenotypic and species data

Phenotypic data were obtained from plants grown under greenhouse conditions to reveal genetic differences among populations and to remove environmental variation. Seeds were obtained from 33 native populations spanning the distribution of *A. gerardii* across the central grasslands (Fig. S1 and Table S3). In 2014, seeds were germinated and grown in SunGro® Metromix® 510 Standard Soil Mix in a greenhouse under natural light. Upon germination, seedlings were separated and transferred individually to pots. Plants were watered to field capacity as needed. We measured fitness-related phenotypic traits: end-of-season aboveground biomass, height, leaf width, and chlorophyll content (the soil-plant analyses development [SPAD]-index calculated from absorption at 650 and 940 nm measured with a Minolta Soil-Plant Analyses Development-502 chlorophyll meter; Caudle, Johnson, Baer & Maricle, 2014). Data on biomass, height, leaf width, and chlorophyll content were taken 144, 28, 48, and 34 days after germination, respectively. Measurements were averaged across ~23 individuals per population prior to use in the PDMs (Table S3). To determine how well phenotypes of plants grown in the greenhouse reflected responses of plants grown in the field despite common conditions experienced by plants in the greenhouse, we calculated the correlation between the heights of field-grown plants (13 sites from Johnson et al., 2015) with mean annual precipitation at those sites.

Species records were obtained from Johnson et al. (2015), TROPICOS, GBIF, VegBank, BISON, and 41 other state and provincial herbaria and museums. The combined data set represented >13,000 records, of which we retained 5,254 after data cleaning. These records comprised 1,432 geographically unique records with high-quality coordinates and an additional 3,822 records georeferenced to the level of a county, parish, district, or municipality ('county-level' records). Full details on record vetting are presented in Appendix S1.

2.3 | Modeling the species' niche

To model the relationship between the species' presences and climate, we used boosted regression trees (BRTs; Elith, Leathwick & Hastie, 2008), MAXENT Ver. 3.3.3k (Phillips, Anderson & Schapire, 2006), and generalized additive models (GAMs). Detailed descriptions of the modeling procedures, including background selection and methods for handling county-level records and for model training and evaluation, are described in Appendix S1. Briefly, we used all records with high-quality coordinates as-is and augmented these with sets of 'pseudopresences', which represented county-level records (Bombi & D'Amen, 2012). For each set, we trained five models for which a geographically distinct group of sites were withheld for model evaluation (Fig. S2). We evaluated model performance using the Continuous Boyce Index, area under the receiver-operator curve, mean F_{pb}, and the point-biserial correlation (see Table S2 for definitions and interpretation). For each of 30 sets of presence/pseudopresences and background sites, we also calculated one additional 'full' model with all presences/pseudopresences and background sites. Across these full models, we calculated the median prediction and used this to predict responses to climate change. We defined the present and future core of the species' range by identifying areas with predictions that fell within the top 2.5th percentile of current predicted values. Using higher (or lower) thresholds decreased (or increased) the core area but indicated qualitatively similar changes in location and direction of shift under climate change.

2.4 | Modeling phenotypic variation

We modeled the relationship between climate variables and mean population biomass, height, leaf width, and chlorophyll content using BRTs and boosted GAMs (Hothorn, Müller, Schröder, Kneib & Brandl, 2011). The response variable in each model was the average phenotypic value for each population. To ensure that the predicted values of responses were >0, we used a gamma error distribution with a log link function (Hothorn et al., 2011). We experimented with including spatially varying coefficients of climate variables but found this produced non-random patterns in the residuals so did not include them in the final models. We adjusted the parameterization for each model based on examination of residuals in predictor space and geographic space (Figs S7–S14).

2.5 | Importance of environmental variables

We evaluated the importance of each variable in the SDM and PDMs using a permutation procedure (Breiman, 2001). First, we made predictions to each site from which seeds were obtained. We then permuted the value of each climate variable in turn and calculated the correlation coefficient between the 'observed' predictions

and predictions with permutation. For the SDMs we used each of the 30 models trained using all presences and averaged results across 100 permutation iterations each. For the PDMs, we averaged results across 100 permutation iterations. Finally, we subtracted the mean correlation coefficient from 1 to create an index of variable importance (Breiman, 2001). Lower values connote less importance because predictions that are relatively unaffected by the variable will be similar to those with the predictor of interest permuted.

2.6 | Extrapolation

To understand the models' behavior when extrapolating beyond current climate conditions, we visually examined response curves for each variable in which each predictor was changed systematically from its minimum to its maximum observed value across North America both now and in future periods while holding the other variables at their median value across the phenotyped populations. We also compared the range of each predictor variable across the phenotyped populations and species to its expected range under scenarios of climate change to determine how well sampling of the phenotype and species covered the range of current and future climate. Finally, we assessed the degree of extrapolation in multivariate climate space by mapping the current location of the future climate expected to predominate in the area from which we phenotyped populations. To do this, we used SDMs in 'reverse', training them with future climate at the locations of phenotyped populations and then projecting the model backward to the present to produce an index of multivariate climatic similarity between the present and future.

3 | RESULTS

Although our results were not strongly affected by extrapolation, we focus on predictions in the geographic region represented by the phenotyped source populations. The BRT and MAXENT SDM algorithms out-performed GAMs for each metric of model performance (Table S2). Both BRTs and Maxent had equivalent performance metrics when tested against geographically distinct hold-out data (Table S2). Likewise, the predicted location and areal coverage of the current core of the distribution (the top 2.5% of predicted values) were very similar between algorithms and in all cases fell within the area covered by the populations that we phenotyped (Figures 1a, S2a, and S3a; mean area $\pm$ *SD* across 30 replicates: $6.7 \pm 0.3 \times 10^5$ km^2 for BRTs, $6.2 \pm 0.4 \times 10^5$ for MAXENT, and $6.8 \pm 0.2 \times 10^5$ km^2 GAMs). However, there was more agreement between the trends predicted by the BRT PDM and BRT SDM than between other combinations of PDM and SDM algorithms. Predictions from the BRT SDM were also similar to geographic responses predicted for crops in the region (some of which fall in the same subtribe as *A. gerardii*) that have current distributions similar to the distribution of *A. gerardii* (Lant, Stoebner, Schoof & Crabb, 2016). For these reasons, we have more confidence in predictions from the BRT SDM. Results from the other SDM algorithms appear in the Appendix S1 (Figs S3 and S4).

Both PDM algorithms (BRTs and GAMs) predicted the current distribution of phenotypic variables well (Figures 2 and S6). They both also predicted a general decline in stature (biomass, height, and leaf width) and little change in chlorophyll content, but the magnitude of predicted change was much larger for GAMs (Fig. S6). Bootstrapped GAMs displayed very erratic fits, demonstrating high sensitivity to data values (Figs S11–S14). As a result, we have more confidence in predictions from the BRT PDMs and therefore focus on results from these models, although regardless of which algorithm used the trends in predictions (increase/decline) were the same. Results for the GAM PDMs are in the Appendix S1 (Fig. S6).

By 2070, the species as a whole and the phenotyped populations are predicted to experience roughly equivalent magnitudes of climate change. Under RCP4.5, the phenotyped populations experience an average increase in mean annual temperature of 3.1°C, while the species' range as a whole (calculated across all presences)

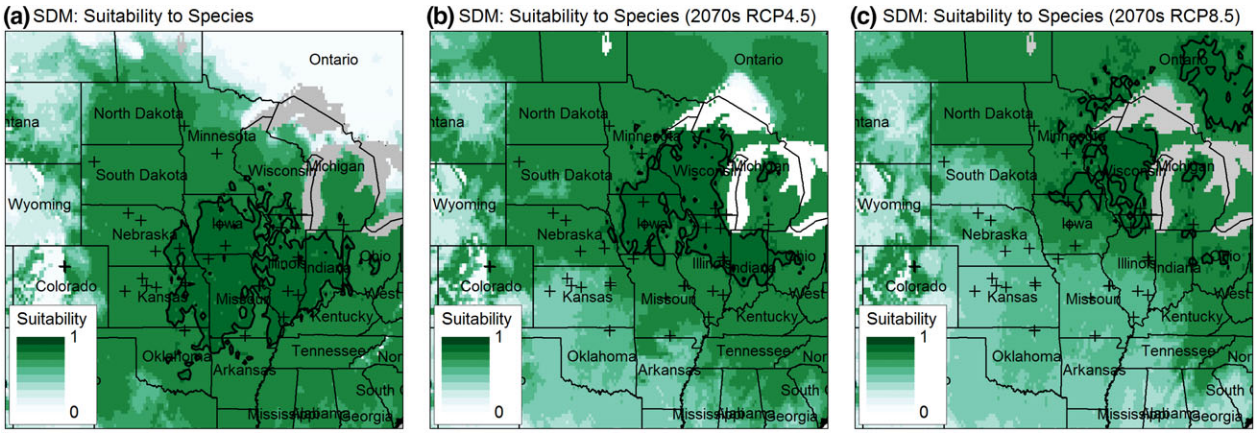

FIGURE 1 Predicted current (a) and future climatic suitability for the dominant prairie grass *Andropogon gerardii* in 2070 for RCP4.5 (b) and RCP8.5 (c) using the BRT algorithm. Crosses represent locations of phenotyped populations. Contour lines represent the core of the species' range (predictions falling in the top 2.5th percentile of current predicted values). Under both future scenarios the core shifts northeast of its current location toward the Great Lakes region

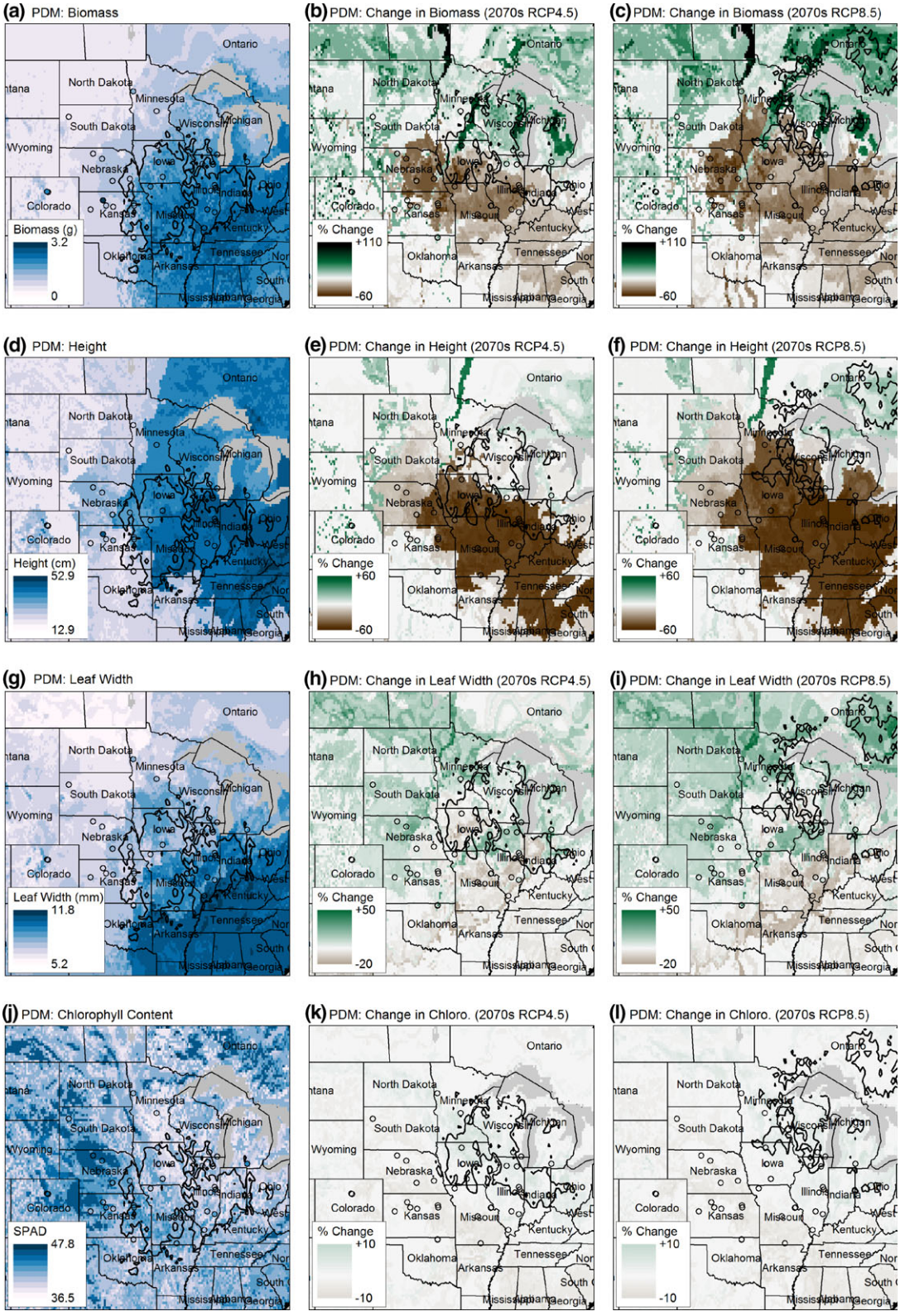

FIGURE 2 Predicted current phenotypic measures (leftmost column) and predicted percent change (middle and right columns) in biomass (a–c), plant height (d–f), leaf width (g–i), and chlorophyll content (j–l) of *Andropogon gerardii* using the BRT algorithm. Percent change is calculated as (100× the future predicted value divided by current predicted value)– 100. Circles denote locations of phenotyped populations. Color scales for the middle and right columns are comparable across traits. Colors of populations in the left panels reflect observed values. Colors of populations in the middle and right panels represent their predicted values. The irregular polygon represents the species-level range core distribution area calculated from the SDM (same as in Figure 1). In general, the area encompassed by the current core of the species' distribution is predicted to suffer large declines in biomass, height, and leaf width

experiences an average increase of 3.0°C. For RCP8.5, the phenotyped populations experience an average increase in mean annual temperature of 4.5°C, while the species' range experiences an increase of 4.4°C. Mean annual precipitation under RCP4.5 declines across phenotyped populations by 16% and across the entire species' range by 10%. Mean annual precipitation under RCP8.5 declines across phenotyped populations by 15% and across the species range by 8%.

3.1 | Species

Currently, the core of the species' range (areas in the top 2.5% of predicted values) extends from northern Arkansas and Oklahoma in the south, through eastern Kansas, Missouri, and Illinois, then northward to southeastern Nebraska, Iowa, and southern Wisconsin (Figure 1a). Under both emissions scenarios, the core distribution area is predicted to shift northeast of its current location into the Great Lakes region of the United States and Canada. Under RCP4.5, the southern edge of the future core overlaps with the northern edge of the current core distribution, while under RCP8.5 there is almost no overlap between current and future core distribution (Figure 1c). Concurrently all but the northeastern side of the current core distribution suffers a general decline in suitability so much that it resembles areas that are currently on the periphery of the species' range.

3.2 | Field vs. greenhouse phenotypes

The height of individual plants grown under field conditions was highly and positively correlated with mean annual precipitation at their region of origin ($r^2 = .78$, $p < 10^{-4}$; Fig. S5), suggesting that responses observed in the greenhouse are largely genetically determined and indicative of the species' response to field (vs. greenhouse) conditions. Nonetheless, actual phenotypic values may differ between field and greenhouse environments. Hence, we focus on proportional change in predicted phenotypic values rather than absolute change under the expectation that the ratio of future to current values is less sensitive to the difference between phenotypic measurements from the greenhouse and the field.

Biomass, height, and leaf width were highly intercorrelated across phenotyped populations ($r \geq .73$ with $p < .001$ in each case), but uncorrelated with chlorophyll content (r between $-.21$ and $-.13$; $p > .2$ in each case).

3.3 | Biomass

Across populations the proportional difference between minimum and maximum mean biomass was 95% ((maximum–minimum)/maximum), ranging from 3.036 g per plant in the eastern part of the core distribution in Illinois to 0.135 g in the western periphery of the range in Colorado. This gradient in biomass was captured by the PDM (Figure 2a–c). Biomass in the current core distribution is predicted to decline by up to ~60% under RCP8.5, although increases up to 10% relative to current values are predicted for the northern central grasslands and the Great Lakes region where the core distribution is predicted to shift.

3.4 | Height

Observed plant height varied by 71% between populations, with stature decreasing from east to west across the central grasslands, a trend also reflected in predictions from the PDM (Figure 2d–f). Under both emissions scenarios, declines in height are predicted for the current core distribution by up to ~60% of current values (especially for RCP8.5). Areas of moderate increase will lie largely north of the current core distribution in the Great Lakes region.

3.5 | Leaf width

Observed leaf width varied by 52% between populations, with width decreasing from southeast to the northwest, a pattern captured by the PDM (Figure 2g–i). Compared to biomass and height, leaf width responded less strongly and had a different geographic pattern of change, showing a decline in the southeast of the current core distribution by up to 20% and an increase in the northwest by up to 50%.

3.6 | Chlorophyll content

Compared with the other phenotypic variables, there was less difference between populations in chlorophyll content, with the minimum mean population value of only 22% less than the maximum (Table S3). Generally, chlorophyll content increased from east to west, although the gradient was more variable compared to other variables (Figure 2j). The PDM predicted chlorophyll content will respond weakly to climate change, declining in the middle of the current core distribution by up to 10% and increasing along the northeastern edge by ≤10% (Figure 2k-l).

3.7 | Importance of environmental variables

The permutation test indicated that maximum temperature of the warmest month had the strongest influence on the distribution of the *A. gerardii* (1 minus correlation between the SDM with predictors as-is vs. predictions with maximum temperature permuted was 0.44; higher values connote greater importance). In contrast, mean annual precipitation was the most important climatic predictor of biomass, height, and leaf width in the PDMs (test statistics from 0.49 to 0.77; Table 1). Patterns in chlorophyll content were best predicted by incoming solar radiation (test statistic 0.77).

3.8 | Extrapolation of predictions

These results are subject to the ability of the SDMs and PDMs to extrapolate into climate space beyond the range of the training data. The current range of the training data for the SDM almost entirely encompassed the expected range of each of climate variable under

TABLE 1 Importance of climatic and spatial predictor variables used in the SDM and PDMs. Values are 1 − *r*, the correlation between predictions at sites with phenotyped populations and predictions at the same sites with each predictor variable permuted in turn. Higher values reflect greater importance of the predictor because predictions in the permuted model are more different from the model with un-permuted predictors. The most important variable for the species and each phenotypic variable are shown in bold

		PDMs			
	SDM	Biomass	Height	Leaf width	Chlorophyll
Diurnal temperature range	0.27	0.00	0.01	0.08	0.04
Maximum temperature of warmest month	**0.44**	0.07	0.37	0.05	0.07
Temperature annual range	0.04	0.01	0.00	0.13	0.03
Mean annual precipitation	0.16	**0.56**	**0.77**	**0.49**	0.01
Potential solar radiation	0.09	0.06	0.02	0.02	**0.77**

any scenario of climate change (Fig. S7–S10), so we expect that the species-level prediction is minimally affected by extrapolation.

The phenotyped populations represent the core distribution plus areas on the western and northern periphery of the range, but not farther south or east. Nonetheless, for three of the five predictors, the phenotyped populations sample nearly all of the environmental range occupied by the species (Figures 3 and S7–S10). For the other two variables, the central grasslands is not expected to experience climates indicative of the 'unsampled' portions of the range of these variables (temperature annual range and mean annual precipitation; Figs S7–S10). Hence, sampling of climate space by the phenotyped populations is either as broad as it could be given the species' distribution or adequate given expected change in climate.

The models do extrapolate beyond the environmental range of the species (and phenotyped populations) in temperature of the hottest month by up to 67% of the current range of this variable across the species (Figs S7–S10). However, within the range of the training data, the PDMs predict a declining trend for all traits in response to higher levels of temperature of the hottest month (Figs S7–S14), and we do not expect this trend to be reversed as temperatures increase. Indeed, other data suggest a diminishing trend with increasing temperatures in the phenotypic variables we examined: in closely related species photosynthesis ceases and pollen loses viability just above the average maximum temperature experienced by the species (~35°C; Herrero & Johnson, 1980), and the productivity of *A. gerardii* declines just south of the southernmost populations we sampled for phenotypic analysis (Epstein et al., 1998). We note that BRTs 'clamp' predictions to the last predicted value when extrapolating outside their training range and thus do not predict further decline/increase. In contrast, GAMs and Maxent (with the settings we used) predict continued decline/increase with extrapolation, but we found these responses to be very erratic (GAMs: Figs S11–S14) or predicted presence in climate much hotter than the species currently occupies (Maxent).

Finally, we found that the current location of climate most similar to conditions expected to prevail across the phenotyped populations in the 2070s lies almost entirely within the region encompassed by the phenotyped populations (Fig. S15). Thus, we expect our models extrapolate only to a minor degree in multivariate climate space.

4 | DISCUSSION

We found that the area of highest climatic suitability of the dominant prairie grass *Andropogon gerardii* is predicted to shift northeastward 700 km or more from the central United States to the Great Lakes region. Concurrently, the current core distribution is predicted to suffer a decline in climatic suitability, with simultaneous declines in biomass and height by up to 60% and leaf width by 20%. Although predicted declines in these traits are dramatic, they fall within the range of phenotypic variation observed across populations of this species and do not necessarily mean that the *A. gerardii* will be eliminated from its current core distribution. The magnitude of reduction in growth-related traits strongly suggests *A. gerardii* could become a less dominant species. Current populations that resemble the phenotypes predicted to be the most suited to the future conditions in the core distribution in Kansas and Missouri presently occur ~800 km westward in the more arid conditions of eastern Colorado. In contrast, areas northeast of the current core distribution (such as in Wisconsin and Michigan) are predicted to become more suitable for large-statured plants currently found ~700 km to the southwest in present-day Kansas and Missouri. Overall our results indicate that decreases in species-level suitability will be manifested by reduced biomass and stature. These predictions have important consequences for prairie restoration (Baer et al., 2016), ecosystem function (Fay et al., 2011), and forage and bioenergy production (Rogler, 1944; Zhang et al., 2015). More broadly, our results demonstrate that to understand species-level dynamics under global change we need to account for intraspecific phenotypic variation of fitness-related traits and how it mediates species' responses to climate change.

4.1 | The fate of the tallgrass prairie ecosystem

Presently, *A. gerardii* plays a dominant role in the core of its range by exerting strong controls over plant diversity (Baer et al., 2016; Collins & Calabrese, 2012) and comprising the majority of aboveground productivity (Rogler, 1944). To some degree, the species is resistant to water stress (Collins et al., 2012) owing to a root system that enables rapid capture of surface water (Nippert, Wieme, Ocheltree & Craine, 2012) and a C_4 photosynthetic pathway that reduces water loss from photorespiration. Nonetheless, *A. gerardii* is not immune to sustained droughts like those that occurred during the

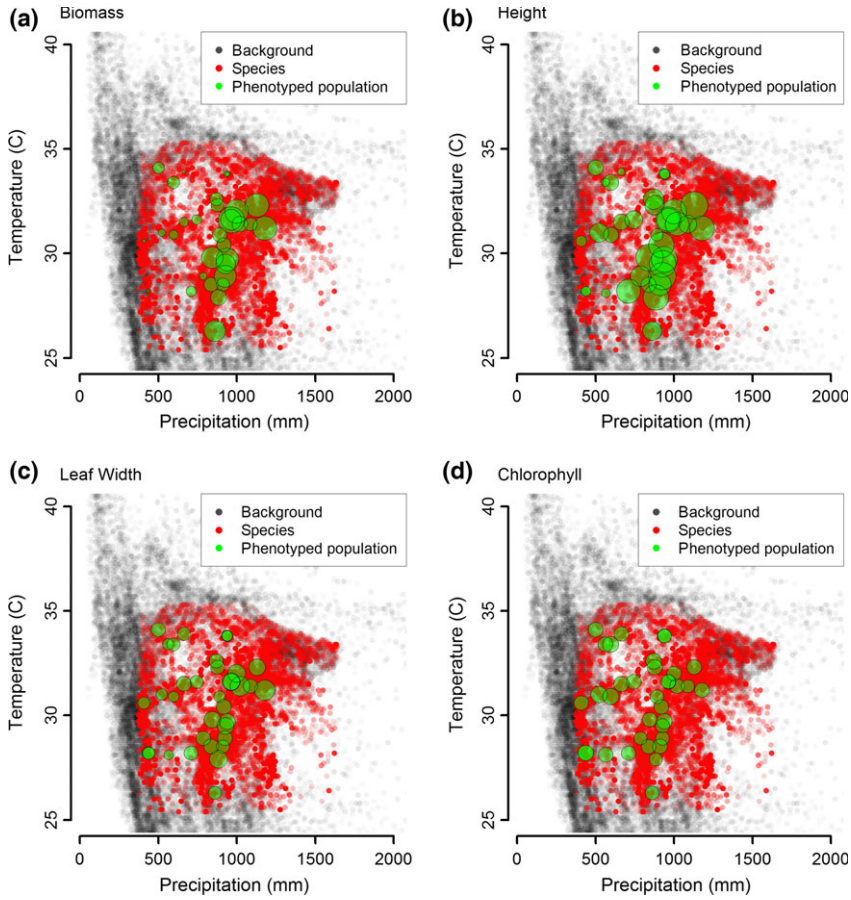

FIGURE 3 Climatic distribution of the species, phenotypes, and available background. The axes represent the two variables that were most important in the PDMs and SDMs, mean annual precipitation and maximum temperature of the hottest month, respectively. The size of points representing phenotyped populations is scaled to the magnitude of each phenotypic variable. Although the phenotyped populations come from a limited geographic distribution, they cover nearly all the environmental space covered by the species. Biomass, height, and leaf width display greater variation across the precipitation gradient than the temperature gradient

1930s 'Dust Bowl' when plants with shorter phenotypes dominated (Weaver & Albertson, 1936). Notably, under greenhouse conditions, plants from drier western and northern populations were smaller than plants from the more mesic south and east (Table S3). The observed phenotypic clines agree with results from reciprocal common garden field experiments (Johnson et al., 2015).

Will *A. gerardii* remain an important species of the central grassland ecosystem? Given that phenotypic variation in this species is in large part genetically controlled (Gray et al., 2014; Johnson et al., 2015; Mendola et al., 2015) and not because of phenotypic plasticity, for several reasons we expect that *A. gerardii* will likely not be able to acclimate or adapt quick enough to future climate conditions. First, most reproduction in this species is asexual through rhizomes' production of clones (Weaver & Fitzpatrick, 1932). Thus, selection has little opportunity to act on variation in propagules produced by outcrossing, thereby obviating rapid adaptive change. Second, dispersal of phenotypes adapted to more favorable climate seems unlikely across the vast distances and fragmented landscape of the prairie ecosystem. Moreover, even if dispersal can effectively deliver appropriately adapted seeds to a site, their establishment might be suppressed by preexisting plants which have greater ability to capture resources owing to larger stature and existing rootstocks which might allow them to persist - albeit in a declining state - as climate becomes unfavorable to them. Based on the phenotypic predictions (Figure 2), we expect existing phenotypes not be matched with climate in their region of origin barring rapid selection, plasticity, and/or gene flow and migration.

These results have important implications for ecosystem services provided by the central grasslands. For example, the US Conservation Reserve Program has restored >2.3 million ha of grassland on what had been marginal agriculture land (USDA Soil Conservation Service 2012). *A. gerardii* is a common component of seed mixes, and dominates many of these restored areas. Currently, cultivars with the closest germplasm origin are generally recommended for these plantings. These results, however, suggest that sourcing seed from geographically more distant populations may be needed to facilitate phenotype-environment matching favored under future climate conditions. For most species, information regarding the geographic distance and environmental conditions defining 'local' is incomplete, so ecological restoration has relied on genetic principles to develop guidelines (Hufford & Mazer, 2003) and a 'best guess' of a species' adaptive potential (Broadhurst et al., 2008). Local population sources have long been advocated for use in

restoration based on logical assumptions that germplasm from nearby environments will establish better in the same climate conditions, exhibit appropriate phenology for provisioning resources to high trophic levels, and minimize the evolutionary risk to nearby natural populations (Hufford & Mazer, 2003). Including non-local sources, however, may be needed to maximize genetic diversity and restored populations' adaptive potential (Broadhurst et al., 2008). Our study suggests collecting germplasm of *A. gerardii* from drier and hotter regions may be needed to restore populations that will be resistant to future conditions in the historically more mesic eastern extent of tallgrass prairie. Local adaptation to soil, however, could hinder non-local genotype matching to environments with favorable climate conditions projected under future emissions scenarios (Mendola et al., 2015).

We encourage thoughtful consideration of human-assisted gene flow (Aitken & Whitlock, 2013) of phenotypes preadapted to changing environmental conditions. Indeed, given that individuals of *A. gerardii* can live up to ~50 year (Keeler, Williams & Vescio, 2002), it may be important to include seeds from preadapted individuals when restoring prairie. However, we emphasize that before assisted gene flow is implemented, several important outstanding questions need to be addressed. Should seeds be sourced exclusively from preadapted populations? If so, which populations (i.e., single populations or mixtures)? Or should source seed represent a mix of both 'local' and preadapted populations? If so, how will preadapted phenotypes perform under current conditions, and will mixing populations lead to mal-adaptive responses in subsequent generations as a result of outcrossing depression? These questions are germane to other ecosystems as well.

4.2 | Intraspecific responses inform species-level responses to global change

Integrating SDMs and PDMs provide a richer understanding of the factors driving species' distributions and functional roles within communities. Whether SDM output is interpreted as a probability of occurrence or an index thereof, it describes only one dimension of potential response to environmental change. However, recent work demonstrates predictions from SDMs correlate with population-level or physiological traits that directly relate to species' persistence and roles within their communities (Michel et al., 2017; Wittmann et al., 2016). Hence, expanding the remit of 'species' distribution modeling to include functional and physiological traits opens promising avenues for forecasting responses to global change (Michel et al., 2017).

Currently, the vast majority of climate vulnerability assessments assume species react to changing climate as if they were homogenous units (Behrman et al., 2014;). The assumption of homogenous response is a convenience ecologists use to make evaluations of climate vulnerability tractable, albeit an assumption belied by numerous studies documenting intraspecific variation (e.g., Behrman et al., 2014; Linhart & Grant, 1996; Malyshev et al., 2016). Other work has demonstrated the power of considering continuous phenotypic variation when evaluating responses to global change. For example, range-wide models that account for differences in growth and mortality across populations demonstrate that a delicate balance between these two forces drives the present and future distributions of Iberian trees, in contrast to standard SDMs that tend to predict a more optimistic future (Benito-Garzón et al., 2013). We expect our approach to be generalizable because many species display phenotypic clines along environmental gradients (Clausen et al., 1940; Etterson, 2004; McMillan, 1959). Indeed, narrow-ranged species are often expected to be more vulnerable to climate change owing to their presumed narrow climatic tolerances, but wide-ranging species often exhibit more phenotypic variation across their ranges (Van Tienderen, 1997). If each phenotype of a widespread species is locally adapted to immediate conditions and unable to track shifting climate thorough adaptation or migration, the species will likely be more vulnerable.

We expect that some correlative SDM algorithms differ in their ability to capture within-species differences. Some methods, like those used here (BRTs, Maxent, and GAMs) are 'local' learners, meaning that they are sensitive to changes in the form of response to different parts of the same environmental gradient. In contrast, other algorithms are less flexible. The ability of locally sensitive algorithms to capture (perhaps unknown) intraspecific variation deserves more attention.

Differences in the importance of climate variables in determining the distribution of the species vs. the phenotype illustrate the opportunity provided by comparing SDMs and PDMs. We found that *A. gerardii*'s distribution is more sensitive to temperature, whereas phenotype is more sensitive to precipitation (Table 1). This suggests different processes determine the overall extent of the range of *A. gerardii* and its phenotype. Indeed, biomass, height, and leaf width vary more across the gradient in precipitation occupied by the species than across temperature (Figure 3). Experimental work has shown that decreasing precipitation affects physiology and water balance but increases in temperature add little to preexisting effects of drought (e.g., Mainali et al., 2014). These studies corroborate the strong relationship between precipitation and phenotype in our PDMs (Table 1). However, these same studies also undermine the importance of temperature in the SDMs. Perhaps, range edges of grasses are especially sensitive to temperature, but given thermal conditions are sufficient within the range, precipitation plays a more influential role in determining variation in productivity (Fay et al., 2011). We hypothesize temperature's effect on phenotype is because of its role in defining the seasonal window for growth and reproduction in this species, while precipitation determines the degree to which the species can take advantage of otherwise favorable temperatures (Fay et al., 2011). More broadly, these results raise the intriguing possibility that range-limiting factors of species are different from factors driving variation in phenotype.

Why would the factors driving species' distributions differ from the factors driving phenotypic distributions? Generally niches are assumed to belong to species, but we posit that they can also belong to trait values. For example, smaller statured individuals are favored in regions with ~400 to ~800 mm of annual precipitation (Figure 3). Above this range, larger individuals are common, while below this

range the species does not occur. We suspect that regions with <~400 mm/yr of precipitation are so dry that were the species to disperse there individuals would be too small to allow sustained resource capture and reproduction, thereby curtailing the species-level distribution (cf. Epstein et al., 1996). In this case, limits on the phenotypic niche constrain the species-level niche. Indeed, traits related to growth and reproduction can impose hard limits on biogeographical distributions by reducing individual fitness (Chuine, 2010).

A combined modeling approach predicts that *A. gerardii* will likely not remain a dominant species in the central grasslands of North America. Our results suggest that the small-statured phenotypes characteristic of the dry western shortgrass prairies will become favored in the current core distribution where tallgrass forms currently predominate. These changes have important implications for diversity and productivity of restored prairies (Collins et al., 2012; Mendola et al., 2015), the livestock industry (Rogler, 1944), and bioenergy production (Zhang et al., 2015). The degree to which the species will actually respond in a manner that matches our predictions depends on the potential for in situ selection (Jump & Peñuelas, 2005; Shaw & Etterson, 2012), sexual reproduction, and dispersal to more suitable sites, perhaps aided by assisted gene flow (Aitken & Whitlock, 2013; Broadhurst et al., 2008; Hufford & Mazer, 2003).

More broadly, our results demonstrate the power and importance of confronting the convenient yet untenable assumption that species always respond homogenously to environmental change. Traditional species-level niche models interpreted at face value can predict very different outcomes than models accounting for intraspecific variation (Behrman et al., 2014; Benito-Garzón et al., 2013; Hällfors et al., 2016). Even when predictions from both types of models coincide, as they do here, PDMs can provide valuable information for conservation, management, and restoration as they can pinpoint phenotypic responses that are fundamental to facilitating expected change (e.g., Michel et al., 2017). This study raises important questions: what phenotypic traits are important for predicting variation in range-wide responses to climate change, and do factors that limit ranges differ from those that determine phenotypic variation?

ACKNOWLEDGEMENTS

We thank Cléo Bertelsmeier, Nora Bello, Camilo Sanín, and two anonymous reviewers for their helpful comments that improved the manuscript. This work was supported by US Department of Agriculture (grant 2008-3510004545 to LCJ and SGB), a grant from the Kansas Academy of Science (JA), and the Alan Graham Fund in Global Change (ABS). The authors declare no conflicts of interest with this study and other interests.

REFERENCES

Aitken, S. N., & Whitlock, M. C. (2013). Assisted gene flow to facilitate local adaptation to climate change. *Annual Reviews of Ecology, Evolution, and Systematics*, *44*, 367–388.

Baer, S. G., Blair, J. M., & Collins, S. L. (2016). Environmental heterogeneity has a weak effect on diversity during community assembly in tallgrass prairie. *Ecological Monographs*, *86*, 94–106.

Behrman, K. D., Keitt, T. H., & Kiniry, J. R. (2014). Modeling differential growth in switchgrass cultivars across the Central and Southern Great Plains. *Bioenergy Resources*, *7*, 1165–1173.

Benito-Garzón, M., Ruiz-Benito, P., & Zavala, M. A. (2013). Interspecific differences in tree growth and mortality responses to environmental drivers determine potential species distributional limits in Iberian forests. *Global Ecology and Biogeography*, *22*, 1141–1151.

Bombi, P., & D'Amen, M. (2012). Scaling down distribution maps from atlas data: A test of different approaches with virtual species. *Journal of Biogeography*, *39*, 640–651.

Breiman, L. (2001). Random forests. *Machine Learning*, *45*, 5–32.

Broadhurst, L. M., Lowe, A., Coates, D. J., Cunningham, S. A., McDonald, M., Vesk, P. A., & Yates, C. (2008). Seed supply for broadscale restoration: Maximising evolutionary potential. *Evolutionary Applications*, *1*, 587–597.

Caudle, K. L., Johnson, L. C., Baer, S. G., & Maricle, B. R. (2014). A comparison of seasonal foliar chlorophyll change among ecotypes and cultivars of *Andropogon gerardii* (Poaceae) by using non-destructive and destructive methods. *Photosynthetica*, *52*, 511–518.

Chuine, I. (2010). Why does phenology drive species distribution? *Transactions of the Royal Society of London B*, *365*, 3149–3160.

Clausen, J., Keck, D. D., Hiesey, W. M. (1940). Experimental studies on the nature of species. I. Effect of varied environments on Western North American Plants. Carnegie Institution of Washington Publication No. 520, Washington, DC.

Collins, S. L., & Calabrese, L. B. (2012). Effect of fire, grazing and topographic variation on vegetation structure in tallgrass prairie. *Journal of Vegetation Science*, *23*, 563–575.

Collins, S. L., Koerner, S. E., Plaut, J. A., Okie, J. G., Brese, D., Calabrese, L. B., … Nonaka, E. (2012). Stability of tallgrass prairie during a 19-year increase in growing season precipitation. *Functional Ecology*, *26*, 1450–1459.

Elith, J., Leathwick, J. R., & Hastie, T. (2008). A working guide to boosted regression trees. *Journal of Animal Ecology*, *77*, 802–813.

Epstein, H. E., Lauenroth, W. K., Burke, I. C., & Coffin, D. P. (1996). Ecological responses of dominant grasses along two climatic gradients in the Great Plains of the United States. *Journal of Vegetation Science*, *7*, 777–788.

Epstein, H. E., Laurenroth, W. K., Burke, I. C., & Coffin, D. P. (1998). Relative productivities of plant species in the Great Plains of the United States. *Plant Ecology*, *134*, 173–195.

Etterson, J. R. (2004). Evolutionary potential of *Chamaecrista fasciculata* in relation to climate change. I. Clinical patterns of selection along an environmental gradient in the Great Plains. *Evolution*, *58*, 1446–1456.

Fay, P. A., Blair, J. M., Smith, M. D., Nippert, J. B., Carlisle, J. D., & Knapp, A. K. (2011). Relative effects of precipitation on variability and warming on tallgrass prairie ecosystem function. *Biogeosciences*, *8*, 3053–3068.

Gray, M. M., St. Amand, P., Akhunov, E. D., Knapp, M., Garrett, K. A., Morgan, T. J., … Johnson, L. C. (2014). Ecotypes of an ecologically dominant grass (*Andropogon gerardii*) exhibit genetic divergence across the U.S. Midwest grasslands' environmental gradient. *Molecular Ecology*, *23*, 6011–6028.

Hällfors, M. H., Liao, J., Dzurisin, J., del Grun, R., Hyvärinen, M., Wi, G. C., & Hellmann, J. J. (2016). Addressing potential local adaptation in species distribution models: Implications for conservation under climate change. *Ecological Applications*, *26*, 1154–1169.

Herrero, M. P., & Johnson, R. R. (1980). High temperature stress and pollen viability of maize. *Crop Science*, *20*, 796–800.

Hijmans, R. J., Cameron, S. E., Parra, J. L., Jones, P. G., & Jarvis, A. (2005). Very high resolution interpolated climate surfaces for global land areas. *International Journal of Climatology*, *25*, 1965–1978.

Hothorn, T., Müller, J., Schröder, B., Kneib, T., & Brandl, R. (2011). Decomposing environmental, spatial, and spatiotemporal components of species distributions. *Ecological Monographs*, *81*, 329–347.

Hufford, K. M., & Mazer, S. J. (2003). Plant ecotypes: Genetic differentiation in the age of ecological restoration. *Trends in Ecology and Evolution*, *18*, 147–155.

Johnson, L. C., Olsen, J. T., Tetreault, H., DeLaCruz, A., Bryant, J., Morgan, T. J., . . . Maricle, B. R. (2015). Intraspecific variation of a dominant grass and local adaptation in reciprocal garden communities along a US Great Plains' precipitation gradient: Implications for grassland restoration with climate change. *Evolutionary Applications*, *8*, 705–723.

Joshi, J., Schmid, B., Caldeira, M. C., Dimitrakopoulos, P. G., Good, J., Harris, R., . . . Lawton, J.H. (2001). Local adaptation enhances performance of common plant species. *Ecology Letters*, *4*, 536–544.

Jump, A. S., & Peñuelas, J. (2005). Running to stand still: Adaptation and the response of plants to rapid climate change. *Ecology Letters*, *8*, 1010–1020.

Kakani, V. G., & Reddy, K. R. (2007). Temperature response of C_4 species big bluestem (*Andropogon gerardii*) is modified by growing carbon dioxide concentration. *Environmental and Experimental Botany*, *61*, 281–290.

Keeler, K. H., Williams, C. F., & Vescio, L. S. (2002). Clone size of *Andropogon gerardii* Vitman (Big Bluestem) at Konza Prairie, Kansas. *American Midland Naturalist*, *147*, 295–304.

Lant, C., Stoebner, T. J., Schoof, J. T., & Crabb, B. (2016). The effect of climate change on rural land cover patterns in the Central United States. *Climatic Change*, *138*, 585–602.

Linhart, Y. B., & Grant, M. C. (1996). Evolutionary significance of local genetic differentiation in plants. *Annual Review of Ecology and Systematics*, *27*, 237–277.

Madakadze, I. C., Stewart, K. A., Madakadze, R. M., & Smith, D. L. (2003). Base temperatures for seedling growth and their correlation with chilling sensitivity for warm-season grasses. *Crop Science*, *43*, 874–878.

Mainali, K. P., Heckathorn, S. A., Wang, D., Weintraub, M. N., Frantz, J. M., & Hamilton, E. W. III (2014). Impact of short-term heat event on C and N relations in shoots vs. roots of the stress-tolerant C_4 grass, *Andropogon gerardii*. *Journal of Plant Physiology*, *171*, 977–985.

Malyshev, A. V., Mohammed, A. S., Khan, A., Beierkuhnlein, C., Steinbauer, M. J., Henry, H. A. L., . . . Kreyling, J. (2016). Plant responses to climatic extremes: Within-species variation equals among-species variation. *Global Change Biology*, *22*, 449–464.

McMillan, C. (1959). Nature of the plant community. V. Variation within the true prairie community-type. *American Journal of Botany*, *46*, 418–424.

Mendola, M. L., Baer, S. G., Johnson, L. C., & Maricle, B. R. (2015). The role of ecotypic variation and the environment on biomass and nitrogen in a dominant prairie grass. *Ecology*, *96*, 2433–2445.

Michel, M. J., Chien, H., Beachum, C. E., Bennett, M. G., & Knouft, J. H. (2017). Climate change, hydrology, and fish morphology: Predictions using phenotype-environment associations. *Climatic Change*, *140*, 563–576.

Nippert, J. B., Wieme, R. A., Ocheltree, T. W., & Craine, J. M. (2012). Root characteristics of C_4 grasses limit reliance on deep soil water in tallgrass prairie. *Plant and Soil*, *355*, 385–394.

Olsen, J. T., Caudle, K. L., Johnson, L. C., Baer, S. G., & Maricle, B. R. (2013). Environmental and genetic variation in leaf anatomy among populations of *Andropogon gerardii* (Poaceae) along a precipitation gradient. *American Journal of Botany*, *100*, 1957–1968.

Phillips, S. J., Anderson, R. P., & Schapire, R. E. (2006). Maximum entropy modeling of species geographic distributions. *Ecological Modelling*, *190*, 231–259.

Polley, H. W., Briske, D. D., Morgan, J. A., Wolter, K., Bailey, D. W., & Brown, J. R. (2013). Climate change and North American rangelands: Trends, projections, and implications. *Rangeland Ecology and Management*, *66*, 493–511.

Rogler, G. A. (1944). Relative palatabilities of grasses under cultivation in the northern Great Plains. *Journal of the American Society of Agronomy*, *35*, 547–559.

Rouse, M. N., Saleh, A. A., Seck, A., Keeler, K. H., Travers, S. E., Hulbert, S. H., & Garrett, K. A. (2011). Genomic and resistance gene homolog diversity of the dominant tallgrass prairie species across the US Great Plains precipitation gradient. *PLoS ONE*, *6*, e17641.

Shaw, R. G., & Etterson, J. R. (2012). Rapid climate change and the rate of adaptation: Insight from experimental quantitative genetics. *New Phytologist*, *195*, 752–765.

Silletti, A., & Knapp, A. (2002). Long-term responses of the grassland co-dominants *Andropogon gerardii* and *Sorghastrum nutans* to changes in climate and management. *Plant Ecology*, *163*, 15–22.

Soil Conservation Service (2012). *Annual summary and enrollment statistics, FY 2012*. Washington, DC: U.S. Department of Agriculture.

Van Tienderen, P. H. (1997). Evolution of generalists and specialists in spatially heterogeneous environments. *Evolution*, *45*, 1317–1331.

Weaver, J. E., & Albertson, F. W. (1936). Effects of the Great Drought on the prairies of Iowa, Nebraska, and Kansas. *Ecology*, *17*, 567–639.

Weaver, J. E., & Fitzpatrick, T. J. (1932). Ecology and relative importance of the dominants of tall-grass prairie. *Botanical Gazette*, *93*, 113–150.

Wittmann, M. E., Barnes, M. A., Jerde, C. L., Jones, L. A., & Lodge, D. M. (2016). Confronting species distribution model predictions with species functional traits. *Ecology and Evolution*, *6*, 873–880.

Zhang, K., Johnson, L., Vara Prasad, P. V., Pei, Z., & Wang, D. (2015). Big bluestem as a bioenergy crop: A review. *Renewable and Sustainable Energy Reviews*, *52*, 740–756.

SUPPORTING INFORMATION

Additional Supporting Information may be found online in the supporting information tab for this article.

How to cite this article: Smith AB, Alsdurf J, Knapp M, Baer SG, Johnson LC. Phenotypic distribution models corroborate species distribution models: A shift in the role and prevalence of a dominant prairie grass in response to climate change. *Glob Change Biol*. 2017;23:4365–4375. https://doi.org/10.1111/gcb.13666

Appendix 1 Climate data, species' records, species-level modeling, and phenotypic modeling

Online supplement to *Phenotypic distribution models corroborate species distribution models: A shift in the role and prevalence of a dominant prairie grass in response to climate change* by Adam B. Smith, Jacob Alsdurf, Mary Knapp, Sara G. Baer, and Loretta C. Johnson.

Contents

Climate data

Climate data was obtained from the WORLDCLIM Version 1.4 Release 3 data set (Hijmans *et al.*, 2005) at 10-arcmin resolution for the periods 1950-2000, 2041-2060, and 2061-2080 for each of two emissions pathways (RCP4.5 and RCP8.5) from the fifth Coupled Model Intercomparison Project (CMIP5). The current climate data is calculated from weather station data that is interpolated using elevation as a covariate (Hijmans *et al.*, 2005). Future climate data is based on the delta method downscaling which subtracts current high-resolution surfaces from future predictions at course grain sizes after resampling the latter to the finer grain (USAID 2014). Future climate surfaces for the WORLDCLIM dataset consists of predictions from 19 global circulation model (GCM) predictions. Of these, we chose 8 and calculated the average monthly precipitation, maximum temperature, and minimum temperature, then from these layers the 19 BIOCLIM variables plus climatic water balance (see main text). We chose these 8 GCMs

because they had predictions for each of the RCPs we were interested in (RCP4.5 and 8.5). Several GCMs were represented by multiple predictions (e.g., HadGEM2-AO, HadGEM2-CC, and HadGEM2-ES). When choosing among these, we gave preference to variants that included the largest number of system components (e.g., HadGEM2-AO models only the troposphere, land surface and its hydrology, aerosols, and ocean/sea-ice dynamics, while Had2GEM-CC models these plus ocean biogeochemistry, and Had2GEM-ES incorporates all of these components plus atmospheric chemistry—and thus was chosen to represent the "HADGEM2" family; Martin *et al.*, 2011).

Solar radiation was calculated using the Potential Incoming Solar Radiation module in SAGA GIS Ver. 2.1.4 (Conrad *et al.,* 2015) and the elevation layer from the WORLDCLIM data set (Hijmans *et al*. 2005).

We also considered climatic water balance (CWB, the difference between precipitation and potential evapotranspiration or PET) and BIOCLIM-like variants of CWB (e.g., CWB of the warmest quarter) but in preliminary analysis found it has as much influence as mean annual precipitation so decided to retain the latter. PET was calculated using a modified, semi-empirical Hargreaves equation that uses mean temperature, precipitation, and latitude as input (Hargreaves et al. 1985; Droogers & Allen 2002).

Table S1. Global circulation models (GCMs) used to create ensemble climate predictions for predicting responses of *Andropogon gerardii* to climate change.

GCM (Abbreviated)	GCM (Full Name)	Representative citation
BCC-CSM1-1	Beijing Climate Center Climate System Model	Xin *et al.*, (2012)
CCSM4	Community Climate System Model	Gent *et al.*, (2011)
GISS-E2-R	Goddard Institute for Space Studies Model	Schmidt *et al.*, (2014)

HadGEM2-ES	UK Met Office Unified Model	Martin *et al.*, (2011)
IPSL-CM5A-LR	Pierre Simon Laplace Institute	Persechino *et al.*, (2013)
MIROC-ESM-CHEM	Model for Japan Agency for Marine-Earth Science and Technology	Watanabe *et al.*, (2011)
MRI-CGCM3	Meteorological Research Institute Model	Yukimoto *et al.*, (2012)
NorESM1-M	Norwegian Earth System Model	Bentsen *et al.*, (2013).

Modeling the species-level niche

Species-level data

We retained all records that matched "*Andropogon gerardii*" (Vitman) and "*Andropogon gerardii* spp. *gerardii*" (hereafter just "*Andropogon gerardii*") that were collected since 1950. When year of collection was ambiguous, we crosschecked the collector with their known dates of activity in the Index of Botanists (Harvard University Herbaria and Libraries, http://kiki.huh.harvard.edu/databases/botanist_index.html).

Records were classified by their coordinate certainty. Many databases have no field for coordinate quality, and those that do often use different systems. Hence, we applied our classification scheme as conservatively as possible, putting records in the lower quality class when in doubt. "High accuracy" records 1) had coordinates that fell within the given county and state, and either were located by GPS or had a coordinate uncertainty less than the resolution of the environmental data (<16 km). "County" records listed a county (or sub-county political district) that fell within the given state or had coordinates that fell within the listed county but there was no state listed and there was but one county in our study region with this name. In some cases we found that county lines had been redrawn or counties had been eliminated since the time of collection, so we assigned location accordingly when possible. We scrutinized records with coordinates pairs reported with no or just one significant digit (e.g., (-101, 37) or (-

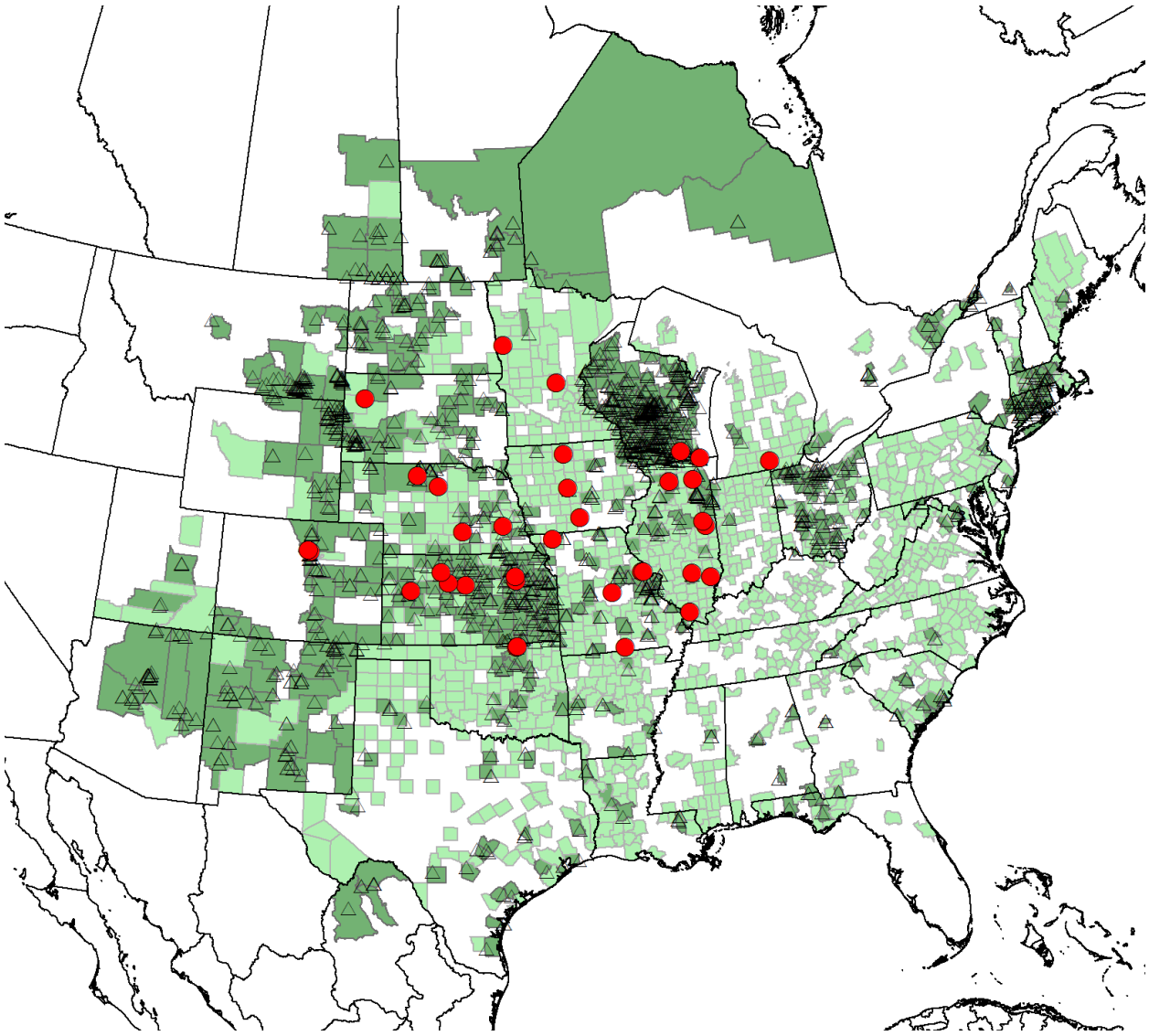

Figure S1. Point- and county-level distribution of records of *Andropogon gerardii* used for species niche modeling. Triangles represent high-quality coordinates and red circles location of phenotyped populations. Counties with colors have ≥1 record within their confines recorded between 1950 and 2014. Darker counties have at least one high-quality record (i.e., a triangle) while lighter counties have at least one county-level record (but no high-quality records).

97.2, 42.1)) since such "truncated" coordinates often indicate imprecise geolocation. All other records were removed. We decided to exclude the disjunct records in the southern Sierra Madre Occidental and the Eje Volcánico Transversal ranges of Mexico because they have unknown affiliations with *A. gerardii* var. *hondurensis* and are geographically closer to that variety than to

A. gerardii var. *gerardii*. In the end we had 1432 geographically unique high-quality records and 3822 county records, out of an initial 13,332. All told, 1755 counties had records, of which 510 (29%) had at least one high-quality record (and possibly county records), and another 1221 (71%) at least one county record (and no high-quality records; Fig. S1).

We used the "envelope" technique described in Bombi & D'Amen (2012) to convert county-level records into "pseudopresences" usable by the SDMs. Specifically, we randomly placed presences in each county with at least one record after masking areas covered by regularly flooded forest and artificial surfaces (though *A. gerardii* is primarily a grassland species, many of our high-quality sites were located in closed forests, so we did not include this land cover type in the mask) and removing areas higher than the 95th percentile of elevations observed at high-quality sites. Land cover was obtained from GlobCover Ver. 2009 (Bontemps *et al*., 2011) and elevation from the 30-arcsec WORLDCLIM data set (Hijmans *et al.*, 2005). To control for county size we placed pseudopresences proportional to collection density in each county. High-quality records were included by representing them multiple times also in proportion to their density within a county. We then drew 10,000 sites from this set to train each SDM. In the US counties tend to be smaller in the East and larger in the West. This gradient in county area could cause a SDM to mistakenly assign greater suitability to a region with small counties because the density of records could be higher than an area just as suitable but with smaller counties. To correct for this presences and pseudopresences were thinned so that no point was within 80 km of another (Radosavljevic & Anderson 2014). We chose this distance because it is half the distance between populations with different ecotypically-based genotypes of the species (Johnson *et al*., 2015), so represents the minimum distance across which the species is locally adapted to the abiotic environment and therefore displays different functional responses. It is also

97 greater than the average distance between nearest-neighbor centroids of counties (~22 km) in our
98 study region.
99 *Species model algorithms*
100 To model the species' current and future niche we used boosted regression trees (BRTs; Elith et
101 al. 2008) and Maxent version 3.3.3k (Phillips *et al.*, 2006; Phillips & Dudík 2008). BRTs fit a
102 sequential set of classification and regression trees (CARTs), each trained on a randomly chosen
103 subset of the training points. An optimal number of trees is chosen based on the number that
104 minimizes out-of-bag deviance from the portion of the data not in the subset used to train the
105 model. The response functions of a BRT model tend to be visually "jagged" in appearance
106 because they are composed of multiple CARTs which divide up the predictor space. Maxent
107 first estimates the probability of observing a set of environmental conditions given the species is
108 present then uses Bayes' rule to invert the probability to generate in index of environmental
109 suitability. We trained BRTs with a learning rate of 0.001, tree depth of 4, bag fraction of 0.7,
110 and a maximum number of trees of 4000, all of which fall within the range suggested by Elith et
111 al. (2008). We trained Maxent with linear, quadratic, and interaction functions to ensure smooth
112 response functions (Elith *et al.*, 2010). Maxent's master regularization parameter was tuned
113 using AIC_c (Warren & Siefert 2011) using custom code in R (available at
114 http://www.earthskysea.org/r-code). For each algorithm we trained 30 SDMs using 30 different
115 versions of background and presence/pseudopresence sites. For each algorithm across these
116 models we calculated the median prediction to use for interpretation.
117 We tested several methods for locating background sites including drawing sites from
118 ecoregions containing or near known presences of *A. gerardii*, using geographically thinned or

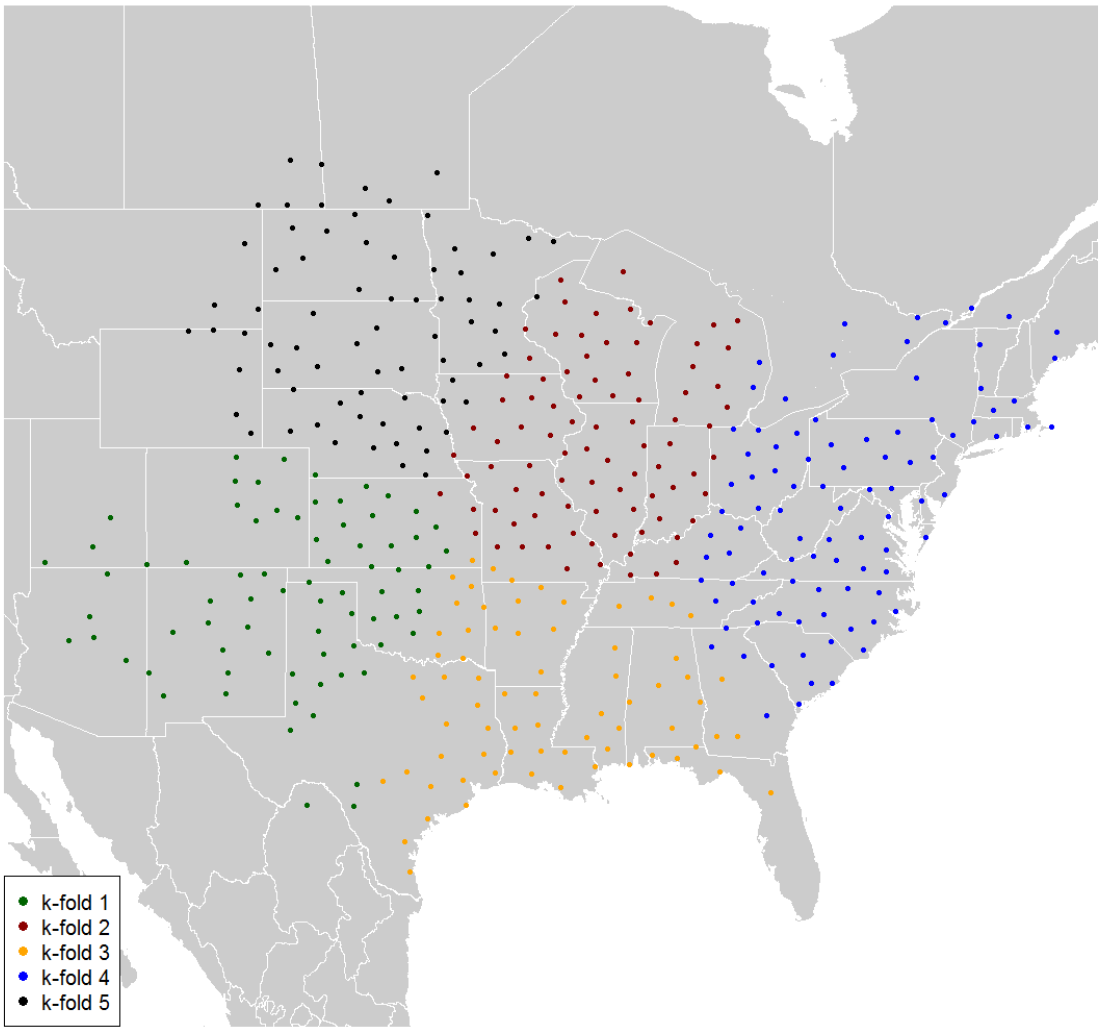

Figure S2. An example of geographically split k-folds or "g-folds" used to train and test a SDM. The model is trained on all but one of the folds and tested on the withheld fold. Each fold is associated with a set of background sites that fall within its confines or closest to it (not shown). These background sites are used along with the fold(s) to train/test the model. Points on the map represent geographically-thinned presences or pseudopresences.

unthinned collections of members of Poaceae obtained from the Global Biodiversity Information Facility (GBIF: http://www.gbif.org/) as target background sites (Phillips *et al.*, 2009), and random selection of sites (drawn proportionally to cell area) from across North America. In the end we decided to use background sites drawn from across the continent because they produced the most plausible current predictions.

SDMs were tested using geographically-stratified test sets of presences and associated background sites, or "g-folds" (Fig. S2). Geographic separation between training and test sites increases their independence, thereby enhancing confidence in performance metrics (Bahn & McGill 2013).

135

Table S2. Relative performance of the three SDM algorithms. BRTs and Maxent out-performed GAMs but otherwise had similar performance. Values represent averages (±sd) across 30 iterations of presences/pseudopresences and background sites split into 5 geographically distinct groups used for testing (Fig. S2). For each metric the model with the highest score is in bold.

SDM	BRT	Maxent	GAM	Definition and Interpretation
AUC_{bg}	**0.731±0.079**	0.726±0.071	0.726±0.077	Area under the receiver-operator curve calculated with background sites in place of absences. Ranges from 0 to 1 with values >0.5 indicating performance better than random. Value represents probability a presence has a higher predicted value than a background site. (Phillips et al. 2006; Elith et al. 2006)
CBI	0.87±0.10	**0.92±0.10**	0.63±0.33	Continuous Boyce Index. Ranges from -1 to 1 with values >0 indicating performance better than random. Represents correlation of model predictions with actual probability of presence. (Boyce et al. 2002; Hirzel et al. 2006)
mean F_{pb}	**0.85±0.10**	0.65±0.10	0.13±0.07	Average value of the harmonic mean of precision (proportion of presence predictions that are correct) and recall (proportion of presences correctly predicted) for thresholds along the sequence 0, 0.01, 0.02, 0.03, …, 1. Range is from 0 to ∞, with higher values connoting better performance. (Li and Guo 2013)
COR	**0.46±0.13**	0.42±0.11	0.40±0.12	Point-biserial correlation, Values range from -1 to 1 with values >0 indicating performance better than random. Represents correlation of model predictions with actual probability of pseudo-presence (i.e., presences vs background sites). (Elith et al. 2006)

136

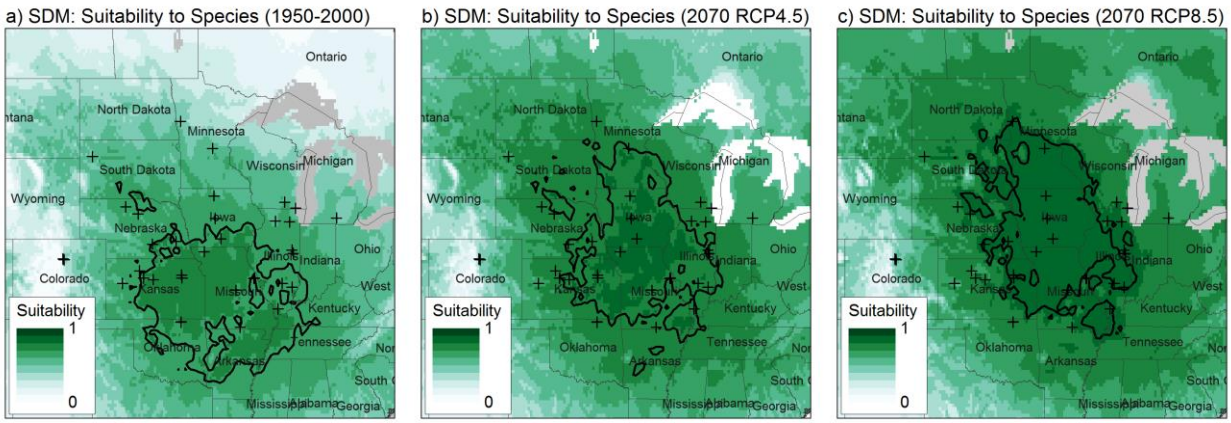

137

138 **Figure S3**. Predicted current (**a**) and future climatic suitability for the dominant prairie grass
139 *Andropogon gerardii* in 2070 for RCP4.5 (**b**) and 8.5 (**c**) using the Maxent algorithm. Crosses
140 represent locations of phenotyped populations. Contour lines represent the core of the species'
141 range (predictions falling in the top 2.5th percentile of current predicted values). Compared to
142 the BRT algorithm (Fig. 1), Maxent predicts a gradual northward shift in the core and an overall
143 increase in suitability.

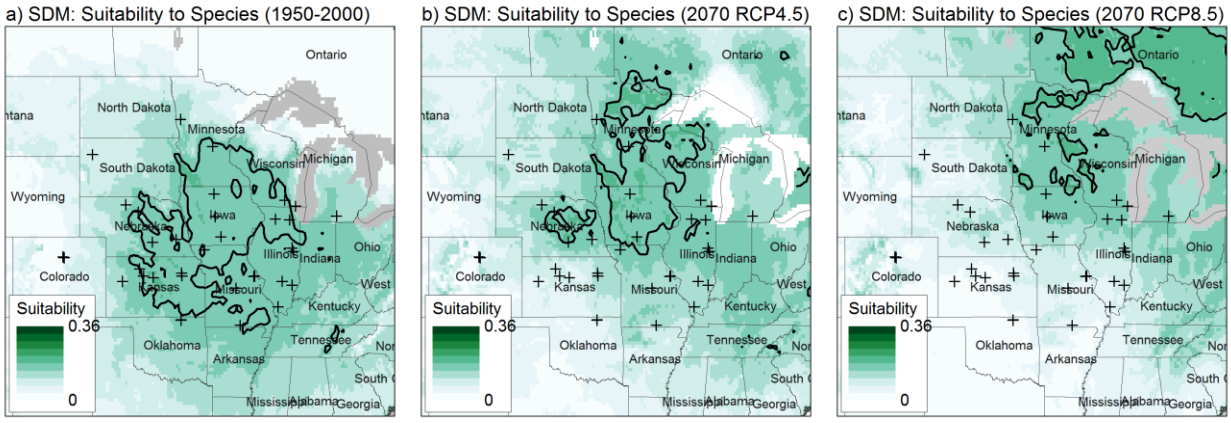

144

145 **Figure S4**. Predicted current (**a**) and future climatic suitability for the dominant prairie grass
146 *Andropogon gerardii* in 2070 for RCP4.5 (**b**) and 8.5 (**c**) using generalized additive models.
147 Despite being more similar to the prediction from BRTs (Fig. 1), GAMs had consistently worse
148 performance than BRTs and Maxent (Table S2).

Modeling phenotypic distributions

Table S3. Location and mean values of the phenotypes of populations used in the phenotype niche models. The first two letters of each population's name refer to the state in which they are located. Two collections were made ~5 km apart at two localities in Nebraska (NE-4 and NE-5, and NE-3 and NE-7), so these were combined and used as one population to avoid overly weighting these sites in the models.

	Traits				Sample Size				Coordinates	
Population	Biomass (g)	Height (cm)	Mean Leaf Width (mm)	SPAD	Biomass	Height	Leaf Width	SPAD	Latitude	Longitude
CO-2	0.2	18.15	7.25	44.55	17	18	18	18	39.99897	-105.284
CO-3	0.521	17.8	7	44.15	15	15	15	15	39.96077	-105.204
IA-2	0.8995	38.15	8.25	37.05	22	22	22	22	43.1431	-93.9454
IA-3	2.526	50.7	9.5	41.4	23	23	23	23	42.01463	-93.8603
IA-4	1.678	47.8	8.5	41.05	21	21	21	21	41.00065	-93.4373
IL-1	1.8585	44.4	11	42.2	22	22	22	22	38.78128	-88.8357
IL-10	2.654	48	9	44.15	23	23	23	23	40.27836	-88.0013
IL-11	1.56	33.4	8	37.2	23	23	23	23	38.59	-88.09
IL-2	2.8175	46	11.5	42.05	22	22	22	22	37.51	-89.14
IL-3	2.545	51.1	8.5	39	23	23	23	23	41.8414	-88.2783
IL-7	2.314	49.8	9.5	40.2	23	23	23	23	40.44512	-88.0979
IL-9	1.55	41.2	7.5	42.6	23	23	23	23	41.88442	-89.3432
KS-10	1.5535	36.35	7.75	43.375	22	22	22	22	39.05	-96.36
KS-13	1.565	38	8	45.65	23	23	23	23	39.2	-96.38
KS-3	0.42	14.7	7.5	40.7	23	23	23	23	38.96607	-98.5111
KS-4	1.387	29.7	8	42.25	23	23	23	23	38.77668	-100.816
KS-8	1.475	29.9	7.5	44.8	23	23	23	23	39.04597	-99.2391
KS-9	0.296	16.1	6.5	42.175	23	23	23	22	39.40198	-99.5425
MI-1	1.892	47.5	10	37.3	23	23	23	23	42.03407	-84.7491
MN-3	1.228	44.65	8	41.3	23	22	23	23	45.51293	-94.0562
MO-3	2.765	51.1	9.5	42.65	23	23	23	23	36.59193	-91.977

MO-4	2.778	46.5	10	41.05	23	23	23	23	38.43859	-92.3094
MO-5	3.036	42.9	9.5	41.35	23	23	23	23	39.0291	-90.961
MO-6	2.431	48	10	39.95	23	23	23	23	39.03783	-90.9091
MO-7	1.715	23.2	6.5	39.25	20	20	20	20	40.35888	-94.6906
ND-1	0.135	16.95	5.5	42.35	21	22	22	22	46.85908	-96.4662
NE-3/NE-7	1.0725	28.9	6	46	46	46	46	46	42.23308	-99.6549
NE-4/NE-5	1.1815	33.7	7.5	42.175	46	46	46	46	40.86996	-96.8058
NE-6	1.083	30.2	8.5	42.9	23	23	23	23	40.73365	-98.5774
NE-8	0.872	35.4	6.5	47.3	23	23	23	23	42.59689	-100.573
OK-1	0.746	21.1	6.5	39.1	23	23	23	23	36.84002	-96.4286
OK-2	0.542	19.7	6	39.95	17	17	17	16	36.86225	-96.4157
SD-1	0.469	20.75	7	41.65	23	22	23	23	45.10292	-103.079
WI-2	2.466	35.4	7.5	38.95	23	23	23	23	42.52812	-87.8242
WI-6	1.673	29	8.5	41.1	17	17	17	17	42.83405	-88.633
MEAN±SE	1.54±0.14	35.03±2.01	8.11±0.24	41.68±0.41						

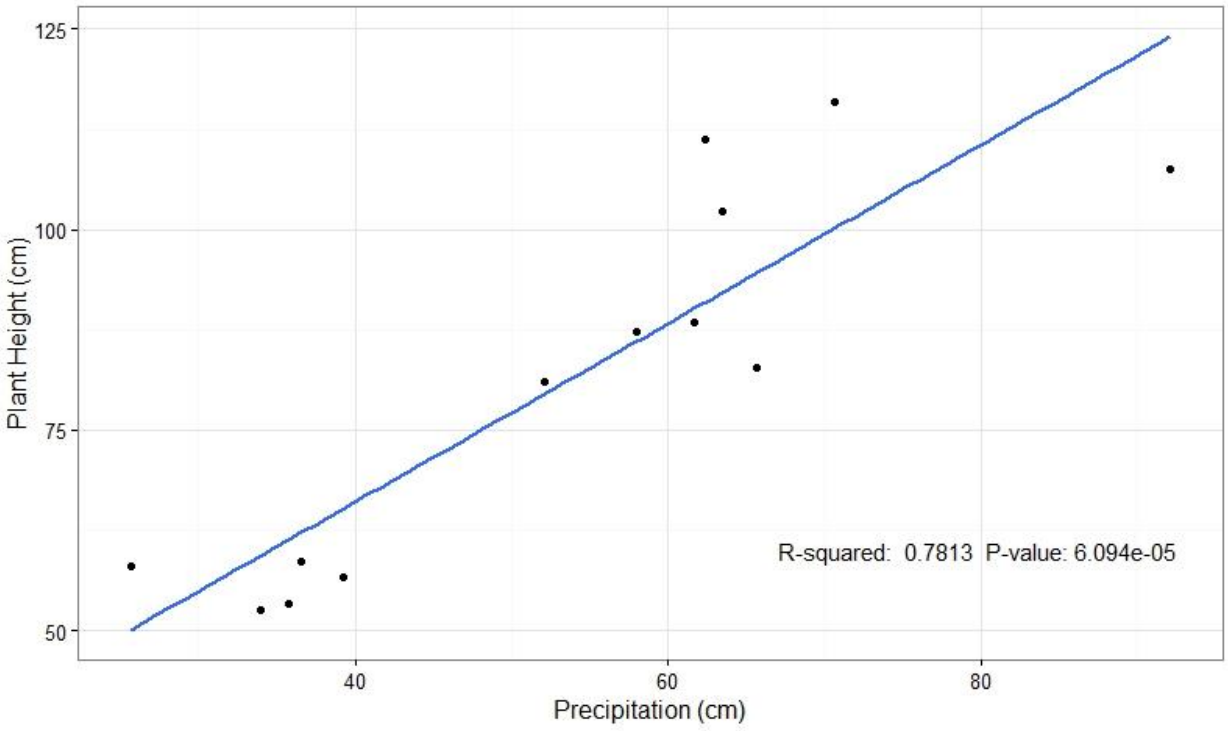

Fig. S5. Relationship between plant height of individuals growing in field conditions and mean annual precipitation. The strong relationship suggests that phenotypic differences observed in the greenhouse are indicative of the climate of source populations.

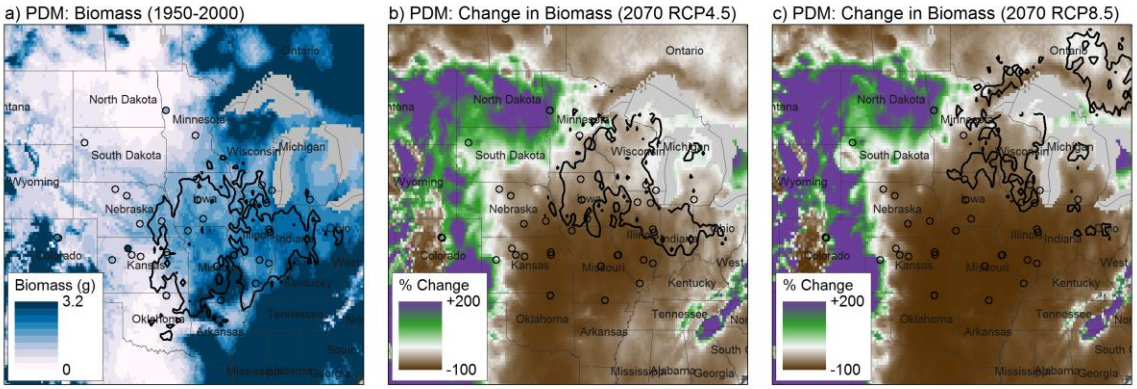

155

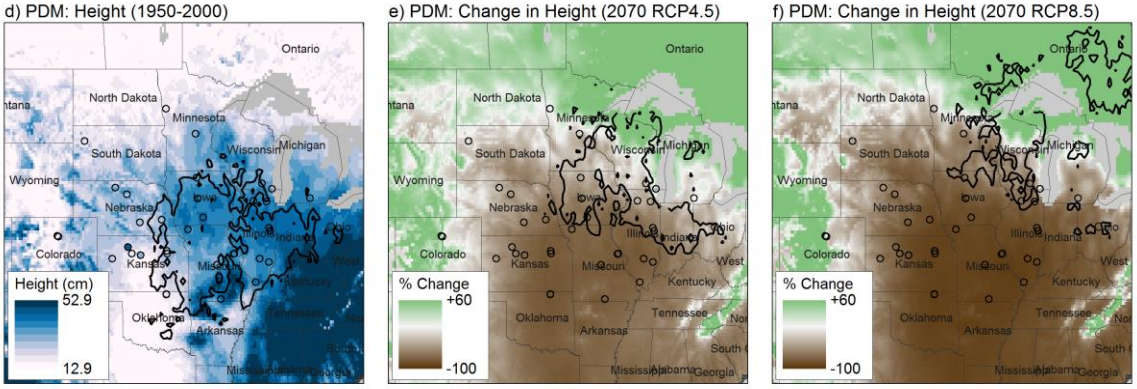

156

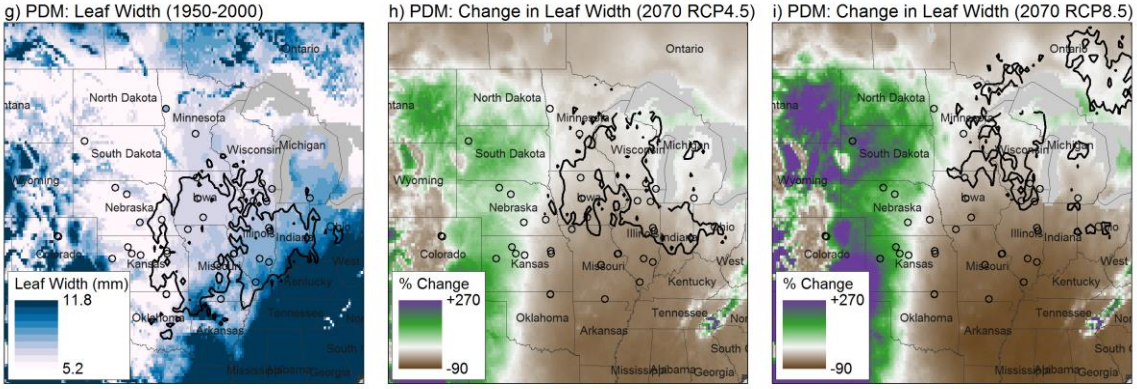

157

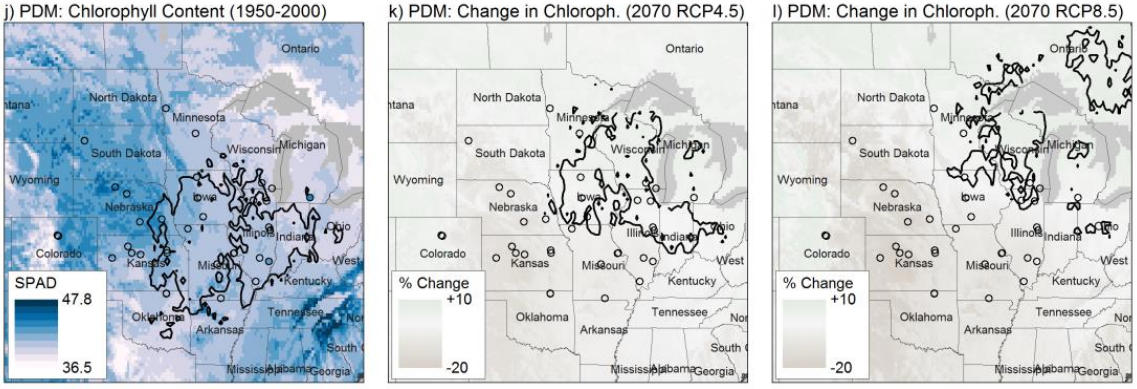

158

Figure S6. Predicted current phenotype (left column) and change in phenotype (middle and right columns) predicted by the GAM PDM model. Geographically the trends predicted by the GAM are qualitatively similar to those predicted by the BRT model (Fig. 2), but the absolute amount of change is much greater due to the manner in which GAMs and BRTs extrapolate beyond the training data. The polygons indicate the current (left column) and future (middle and right columns) core of the species-level distribution predicted by the BRT SDM (Fig. 1).

Model diagnostics

Figure S7 through S10.. Response curves from the phenotype distribution model for each phenotypic variable using the BRT algorithm. In each panel points represent observed values of the given phenotypic variable. Thin gray lines represent predictions from each of 30 bootstrapped PDMs and the black line the prediction from the model using all data as-is (the model used to predict future phenotype). Arrows at the top of each panel represent the current range of the given environmental variable across the species (thick red arrow) and the future range across any future climate scenario (thin red arrow). The thick blue arrow represents the current environmental range occupied by the phenotyped populations and the thin blue line the range occupied across any future climate scenario. WC02 is mean diurnal temperature range, WC05 is mean maximum temperature of the warmest month, WC07 is temperature annual range, WC12 is mean annual precipitation, WC15 is precipitation seasonality, and solarRad is potential incoming solar radiation. In each case the phenotyped populations fully sample the distribution of each climate variable currently experienced by the species or (in the case of WC12) sample the part relevant to future predictions (i.e., the central grasslands are not expected to become wetter under future climate scenarios). Compared to GAMBOOST fit curves were less erratic (see Figs. S11 through S14).

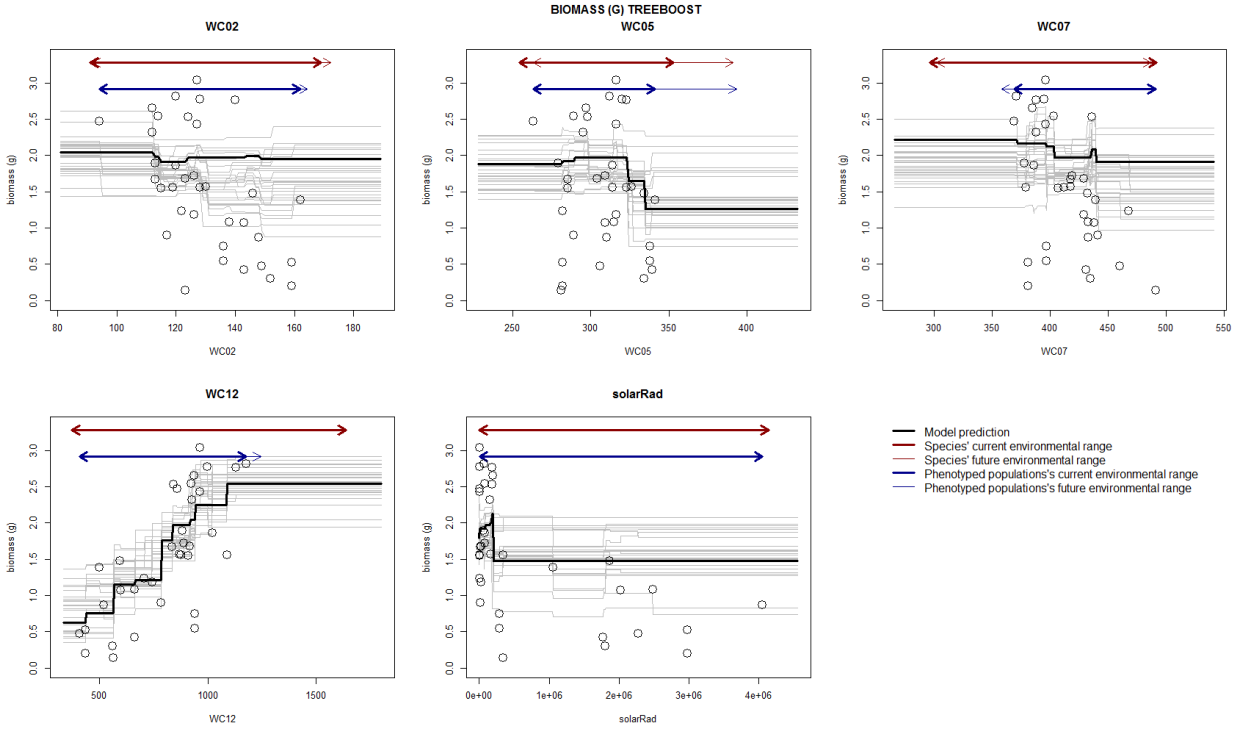

183

184 **Figure S7**. Biomass modeled with BRTs.

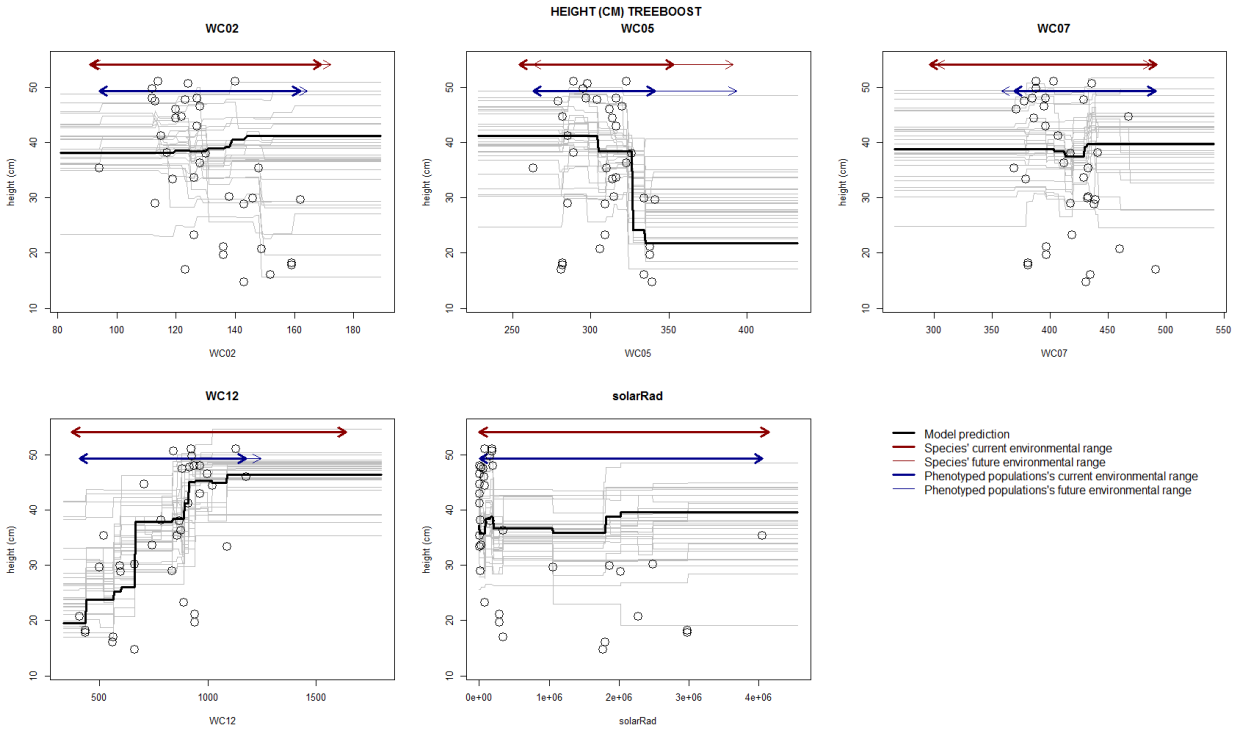

185

186 **Figure S8**. Height modeled with BRTs.

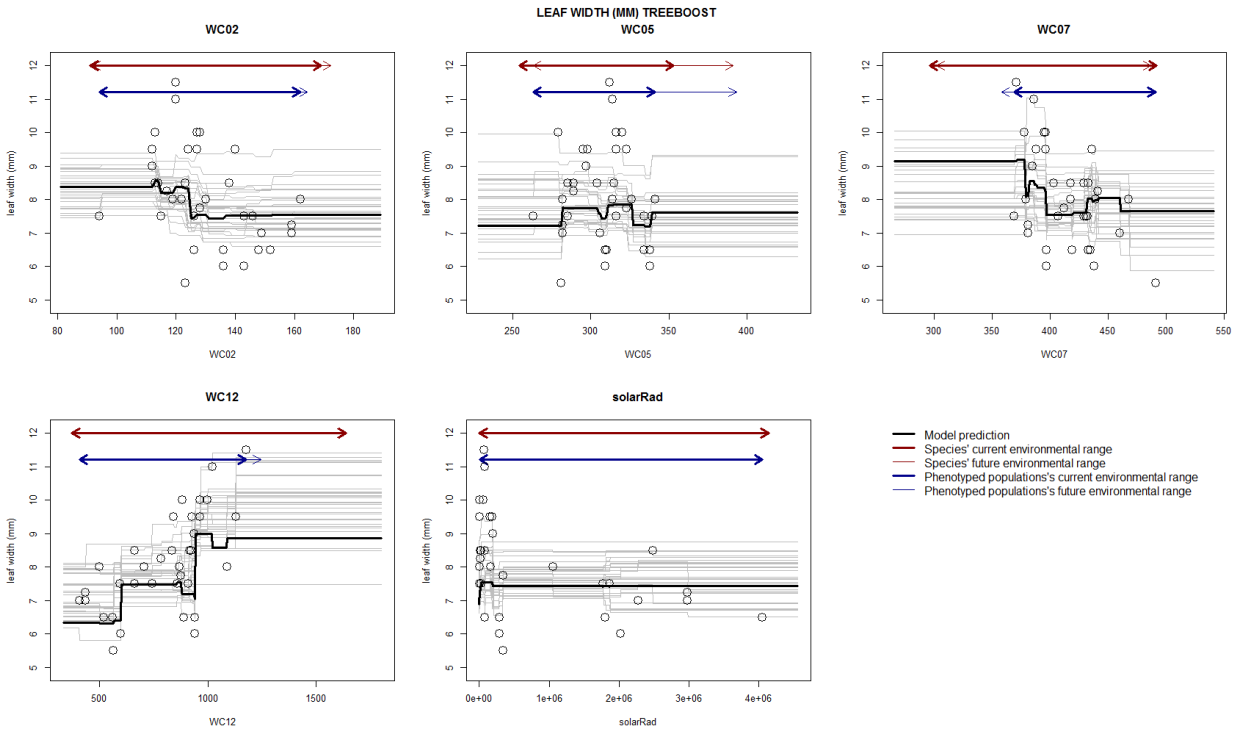

187

188 **Figure S9**. Leaf width modeled with BRTs.

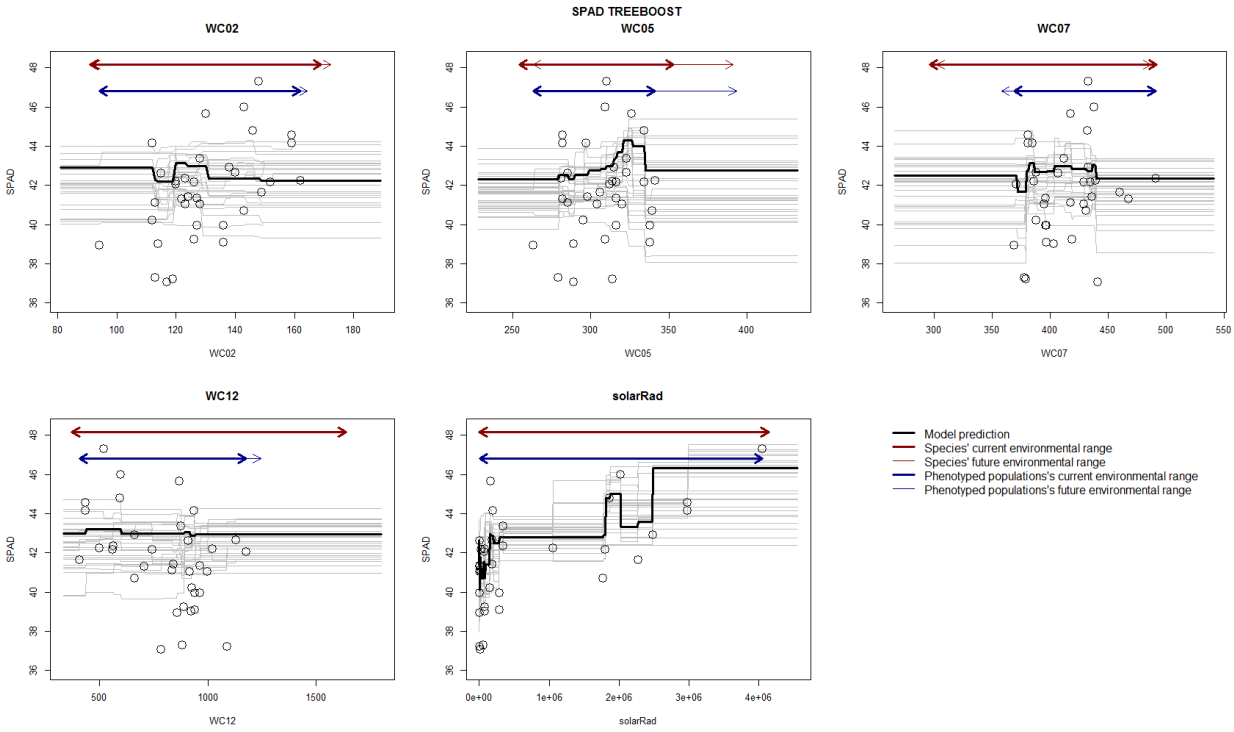

189

190 **Figure S10**. Photosynthetic capacity (SPAD) modeled with BRTs.

Figure S11 through S14.. Response curves from the phenotype distribution model for each phenotypic variable using the GAM algorithm. See caption for Figs. S7 through S10 for further explanation.

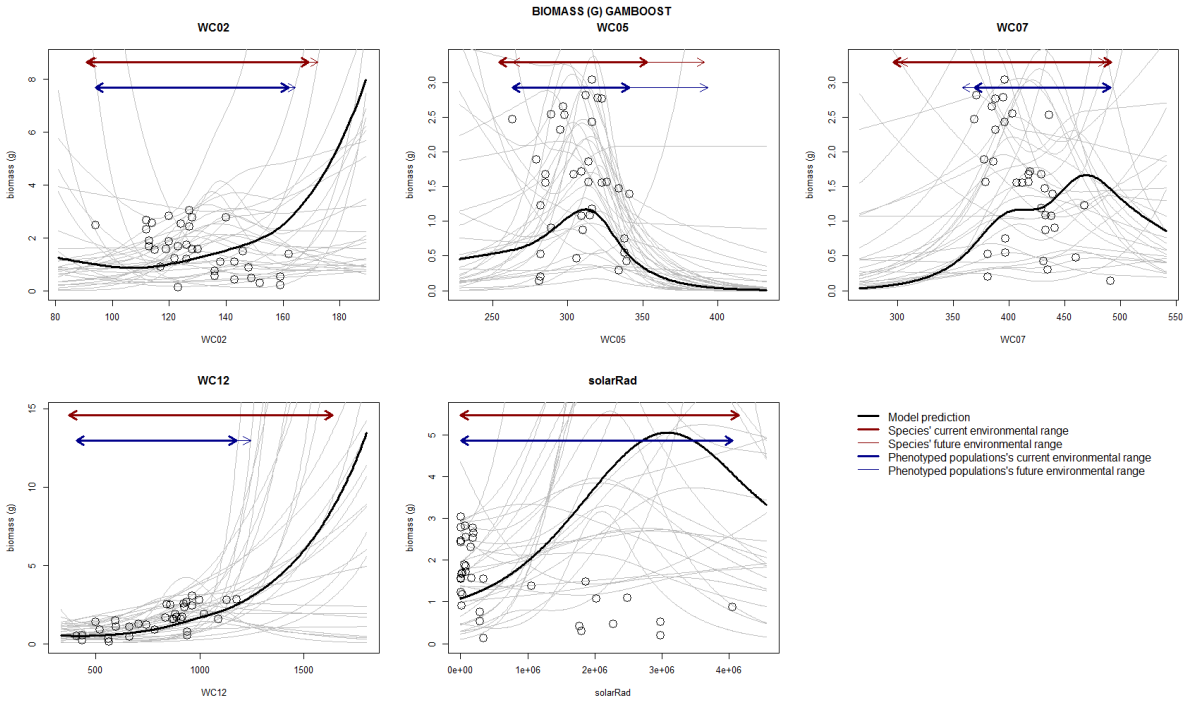

Figure S11. Biomass modeled with GAMs.

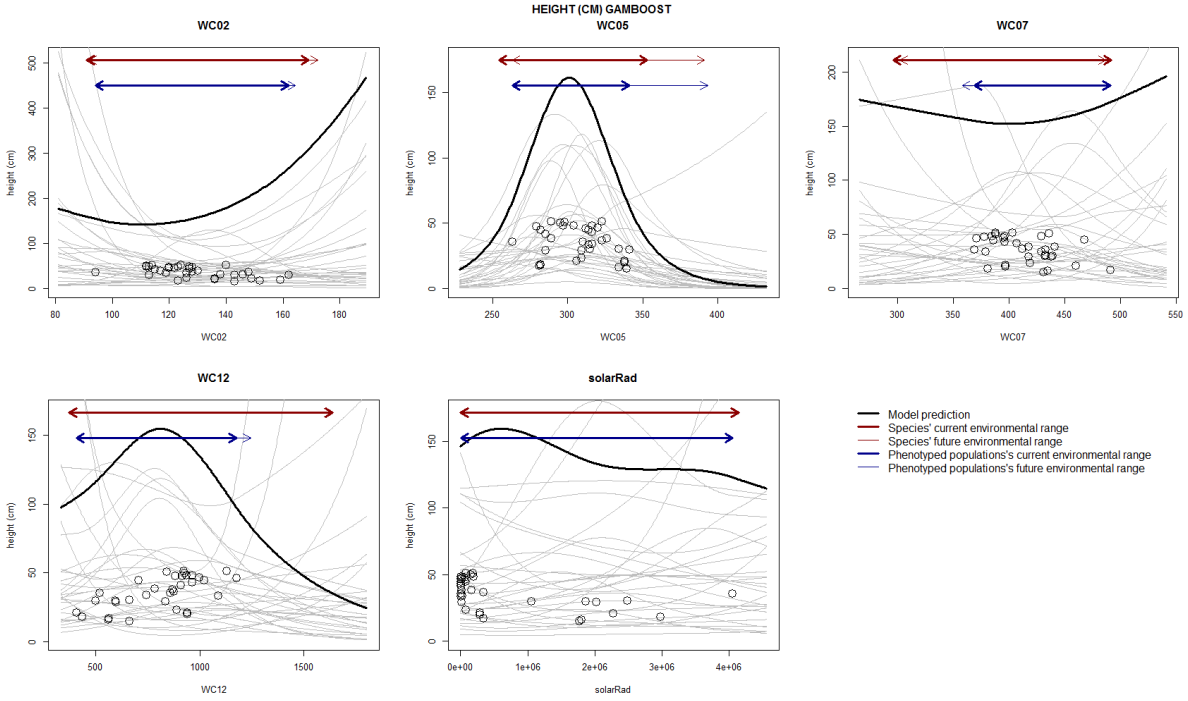

Figure S12. Height modeled with GAMs.

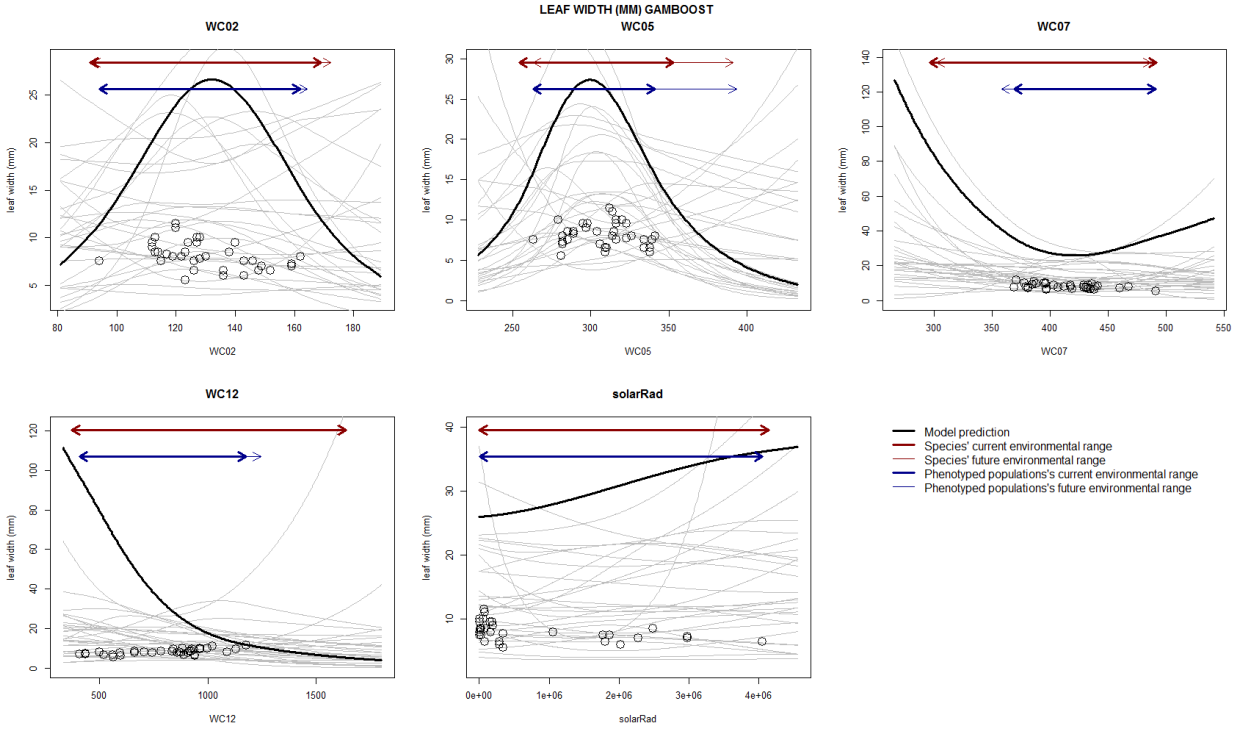

198

199 **Figure S13**. Leaf width modeled with GAMs.

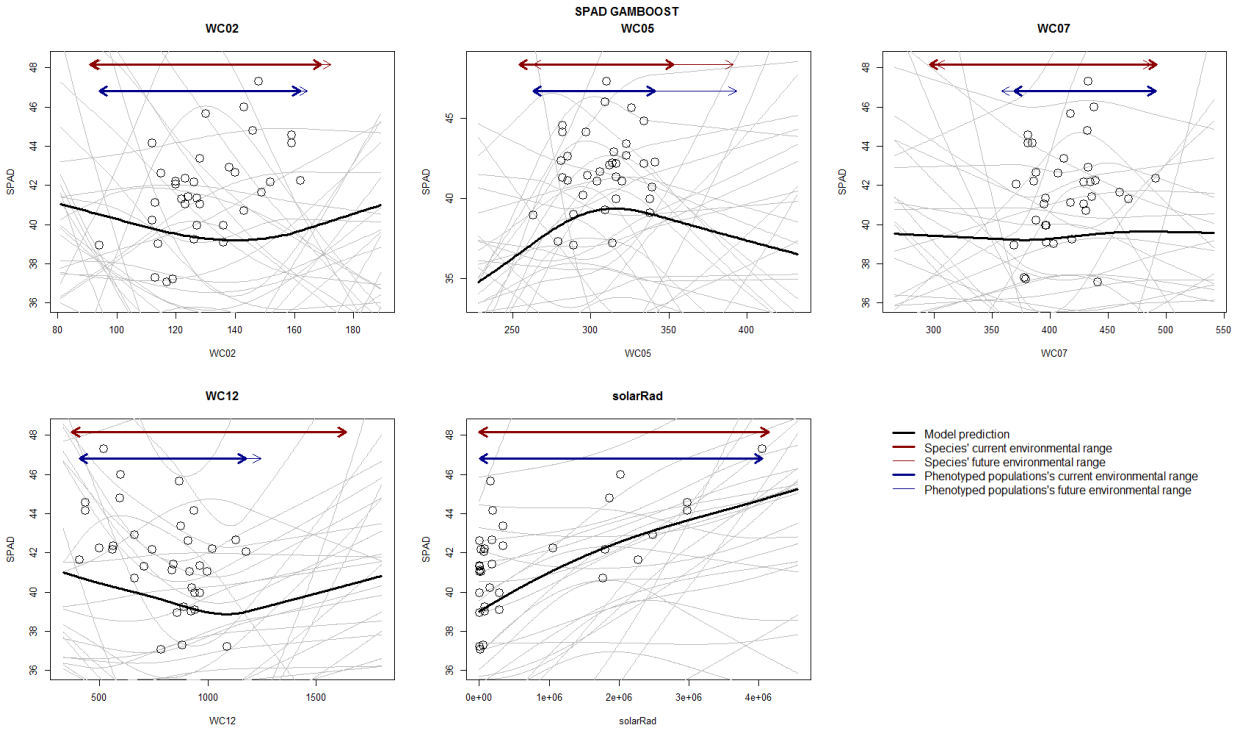

200

201 **Figure S14**. Photosynthetic capacity (SPAD) modeled with GAMs.

Extrapolation in multivariate climate space

Although analysis of extrapolation variable-by-variable suggested that the PDMs were not affected by the limited geographic range of the phenotyped populations, we were concerned that the PDMs might extrapolate into multivariate space that 1-dimensional (Figs. S7 through S10) or 2-dimensional (Fig. 3) analysis might not reveal. Thus we used SDMs in "reverse" to map the current location of the climate most similar to that expected for the phenotyped populations by the 2070s under RCP8.5. Importantly, SDMs operate in climatic space, not geographic space, and as such condense multivariate climate space to a one-dimensional metric of similarity between training presences (or sites used in place of presences) and any set of climate layers into which the model is projected. Thus SDMs actually yield a measure of climatic similarity that can be used to examine the location of climatically similar areas between time periods. We used this technique to map the location of the climate that occurs in the present but is most similar to multivariate climate space the phenotyped populations are expected to experience in the future. We surmised that if the current location of the most climatically similar area was within the geographic range of the populations then the PDM would be affected minimally by extrapolation in multivariate space.

We created a 160-km buffer around the phenotyped populations (the distance across which phenotypic and genotypic differences have been demonstrated to exist in this species; Gray et al., 2014; Johnson et al., 2015) and from this area extracted climate data from RCP4.5 and 8.5 for the 2070s at 1000 randomly-located points. We then trained a Maxent model on this data and climate data from 10,000 randomly located background points located across North America.

The models were then projected to the present using climate layers representing 1950-2000 and mapped.

For both emission scenarios the present location of climate space that is most similar to the climate expected to predominate in the future in the area of the phenotyped populations falls almost entirely within the region covered by the phenotyped populations (Fig. S15). Thus the PDMs are likely nominally affected by extrapolation in multivariate climate space.

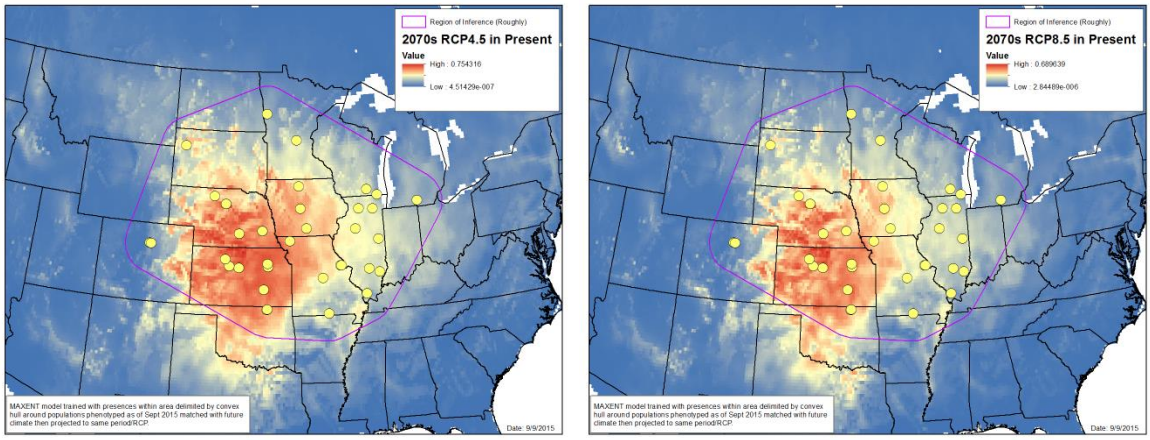

Figure S15. Multivariate climatic similarity between the present (1950-2000) and conditions expected under RCP4.5 (left) and RCP8.5 (right) in the 2070s. Hotter values indicate greater similarity between present-day climate experienced by phenotyped populations and the climate thee populations are expected to experience under the each scenario. For both emission scenarios the most similar current climate to future climate lies within the bounds of the phenotyped populations.

Supplemental literature cited

Bahn, V. and McGill, B.J. 2013. Testing the predictive performance of distribution models. Oikos 122:321-331.

Bentsen, M., Bethke, I., Debernard, J.B., Iversen, T., Kirkevåg, A., *et al.*, 2013. The Norwegian Earth System Model, NorESM1-M – Part 1: Description and basic evaluation of the physical climate. Geoscience Model Development 6:687-720.

Bombi, P. and D'Amen, M. 2012. Scaling down distribution maps from atlas data: A test of different approaches with virtual species. Journal of Biogeography 39:640-651.

Bontemps, S., Defourny, P., Van Bogaert, E., Arino, O., Kalogirou, V., and Perez, J.R. 2011. GLOBCOVER 2009: Products description and validation report. Université catholique de Louvain and European Space Agency.

Boyce, M.S., Vernier, P.R., Nielsen, S.E., and Schmiegelow, F.K.A. 2002. Evaluating resource selection functions. Ecological Modeling 157:281-300.

Conrad, O., Bechtel, B., Bock, M., Dietrich, H., Fischer, E., Gerlitz, L., Wehberg, J., Wichmann, V., and Boehner, J. 2015. System for Automated Geoscientific Analyses (SAGA) v. 2.1.4. Geoscientific Model Development 8:1991-2007.

Droogers, P. and R.G. Allen. 2002. Estimating reference evapotranspiration under inaccurate data conditions. Irrigation and Drainage Systems 16:33-45.

Elith, J., C.H. Graham, R.P. Anderson, M. Dudik [Dudík], S. Ferrier, A. Guisan, R.J. Hijmans, F. Huettmann, J.R. Leathwick, A. Lehmann, J. Li, L.G. Lohmann, B.A. Loiselle, G. Manion, C. Moritz, M. Nakamura, Y. Nakazawa, J.McC. Overton, A.T. Peterson, S.J. Phillips, K. Richardson, R. Scachetti-Pereira, R.E. Schapire, J. Soberon [Soberón], S. Williams, M.S. Wisz, and N.E. Zimmermann. 2006. Novel methods improve prediction of species' distributions from occurrence data. Ecography 29:129-151.

Elith, J., J.R. Leathwick, and T. Hastie. 2008. A working guide to boosted regression trees. Journal of Animal Ecology 77:802-813.

Elith, J., M. Kearney, and S. Phillips. 2010. The art of modeling range-shifting species. Methods in Ecology and Evolution 1:330-342.

Gent, P.R., Danabasoglu, G., Donner, L.J., Holland, M.M., Hunke, E.C., Jayne, S.R., Lawrence, D.M., Neale, R.B., Rasch, P.J., Vertenstein, M., Worley, P.H., Yang, Z-L., and Zhang, M. 2011. The Community Climate System Model Version 4. Journal of Climate 24:4973-4991.

Gray, M.M., St. Amand, P., Akhunov, E.D., Knapp, M., Garrett, K.A., Morgan, T.J., Baer, S.G., Maricle, B.R., and Johnson, L.C. 2014. Ecotypes of an ecologically dominant grass (Andropogon gerardii) exhibit genetic divergence across the U.S. Midwest grasslands' environmental gradient. Molecular Ecology 23:6011-6028.

Hargreaves, G.L., Hargreaves, G.H. and Riley, J.P. 1985. Irrigation water requirements for Senegal River Basin. Journal of Irrigation and Drainage Engineering 111:265-275.

Hijmans, R.J., Cameron, S.E., Parra, J.L., Jones, P.G., and Jarvis, A. 2005. Very high resolution interpolated climate surfaces for global land areas. International Journal of Climatology 25:1965-1978.

Hirzel, A.H., Le Lay, G., Helfer, V., Randin, C., and Guisan, A. 2006. Evaluating the ability of habitat suitability models to predict species presences. Ecological Modeling 199:142-152.

Johnson, L.C., Olsen, J.T., Tetreault, H., DeLaCruz, A., Bryant, J., Morgan, T.J.,Knapp, M., Bello, N.M., Baer, S.G., and Maricle, B.R. 2015. Intraspecific variation of a dominant grass and local adaptation in reciprocal garden communities along a US Great Plains' precipitation gradient: Implications for grassland restoration with climate change. Evolutionary Applications 8:705-723.

Li, W. and Guo, Q. 2013. How to assess the prediction accuracy of species presence-absence models without absence data? Ecography 36:788-799.

Martin, G.M., Belloiun, N., Collins, W.J., Culverwell, I.D., Halloran, P.R., *et al.*, 2011. The HadGEM2 family of Met Office Unified Model climate configurations. Geoscience Model Development 4:723-757.

Persechino, A., Mignot, J., Swingedouw, D,. Labetoulle, S., and Guilyardi, E. 2013. Decadal predictability of the Atlantic meridional overturning circulation and climate in the IPSL-CM5A-LR model. Climate Dynamics 40:2539-2380.

Phillips, S.J. and Dudík, M. 2008. Modeling species distributions with Maxent: New extensions and a comprehensive evaluation. Ecography 31:161-175.

Phillips, S.J., Anderson, R.P., and Schapire, R.E. 2006. Maximum entropy modeling of species geographic distributions. Ecological Modelling 190:231-259.

Phillips, S.J., Dudík, M., Elith, J., Graham, C.H., Lehmann, A., Leathwick, J., and Ferrier, S. 2009. Sample selection bias and presence-only distribution models: Implications for background and pseudo-absence data. Ecological Applications 19:181-197.

Radosavljevic, A. and Anderson, R.P. 2014. Making better Maxent models of species distributions: complexity, overfitting and evaluation. Journal of Biogeography 41:629-643.

Schmidt, Kelley, M., Nazarenko, L., Ruedy, R., Russell, G.L., Aleinov, I., *et al.*, 2014. Configuration and assessment of the GISS ModelE2 contributions to the CMIP5 archive. Journal of Advances in Modeling Earth Systems 6:141-184.

USAID. 2014. A review of downscaling methods for climate change projections: African and Latin American resilience to climate change. USAID Contract No. AID-EPP-I-00-06-00008, Order Number AID-OAA-TO-11-00064.

Warren, D.L. and S.N. Siefert. 2011. Ecological niche modeling in Maxent: The importance of model complexity and the performance of model selection criteria. Ecological Applications 21:335-342.

Watanabe, S. Hajima, T., Sudo, K., Nagashima, T., Takemura, T., Okajima, H., Nozawa, T., Kawase, H., Abe, M., Yokohata, T., Ise, T., Kato, E., Takata, K., Emori, S., and Kawamiya, M. 2011. MIROC-ESM 2010: model description and basic results of CMIP5-20c3m experiments. Geoscience Model Development 4:845-872.

Xin X., Wu T., and Zhang J. 2012. Introductions to the CMIP 5 simulations conducted by the BCC climate system model. Climate Dynamics 38:725-744.

Yukimoto, S., Adachi, Y., Hosaka, M., Sakami, T., Yoshimura, H., Hirabara, M., *et al.*, 2012. A new global climate model of the Meteorological Research Institute: MRI-CGCM3—Model description and basic performance. Journal of the Meteorological Society of Japan 90A:23-64.